INTERNATIONAL ATOMIC ENERGY AGENCY
UNITED NATIONS EDUCATIONAL, SCIENTIFIC AND CULTURAL ORGANIZATION
INTERNATIONAL CENTRE FOR THEORETICAL PHYSICS
I.C.T.P., P.O. BOX 586, 34100 TRIESTE, ITALY, CABLE: CENTRATOM TRIESTE

H4.SMR/942-21

**Third Workshop on
3D Modelling of Seismic Waves Generation
Propagation and their Inversion**

**4 - 15 November 1996**

# *Seismic Zoning*

F. Vaccari

Dept. of Earth Sciences
University of Trieste
Trieste, Italy

*Journal of Applied Geophysics*, 30 (1993) 149–160
Elsevier Science Publishers B.V., Amsterdam



# Zoning of the Italian territory in terms of expected peak ground acceleration derived from complete synthetic seismograms

Giovanni Costa[a], Giuliano Francesco Panza[a,c], Peter Suhadolc[a] and Franco Vaccari[a,b,1]
[a]*Istituto di Geodesia e Geofisica, Università degli Studi di Trieste, Via dell'Università 7, 34100 Trieste, Italy*
[b]*CNR, Gruppo Nazionale per la Difesa dai Terremoti, Roma, Italy*
[c]*International Center for Theoretical Physics, Strada Costiera 11, 34100 Trieste, Italy*

(Accepted after revision September 30, 1992)

ABSTRACT

Costa, G., Panza, G.F., Suhadolc, P. and Vaccari, F., 1993. Zoning of the Italian territory in terms of expected peak ground acceleration derived from complete synthetic seismograms. In: R. Cassinis, K. Helbig and G.F. Panza (Editors), Geophysical Exploration in Areas of Complex Geology, II. J. Appl. Geophys., 30: 149–160.

An automatic procedure for the seismic zonation of a territory is presented. The results consist of deterministic computation of acceleration time series distributed on a regular grid over the territory. For the estimation of the accelerations, complete synthetic seismograms are computed by the modal summation technique. A first rough zonation can be accomplished by considering a map showing the distribution of peak ground acceleration. In this work the new procedure has been applied to the Italian territory. The structural and source models necessary to compute the synthetic signals have been fixed after an extensive bibliographic research. Seismogenic areas have been defined in the framework of the GNDT (Gruppo Nazionale per la Difesa dai Terremoti of the Consiglio Nazionale delle Ricerche, Rome) research activities dedicated to the definition of the kinematic model of Italy. Information on historical and recent seismicity has been taken from the most updated Italian earthquake catalogues. The estimated peak ground accelerations have been found to be compatible with available data, both in terms of intensity (historical earthquakes) and accelerations (recent earthquakes).

## Introduction

The zonation of a territory in terms of seismic hazard is an essential preventive countermeasure in countries with high seismic risk, especially for densely populated areas. Maximum expected peak ground acceleration (PGA), at different frequencies, is a very important parameter considered by civil engineers when designing or reinforcing constructions.

We have developed a deterministic procedure which allows us to estimate PGA (routinely at frequencies as high as 10 Hz) starting from the available information on Earth structure parameters, seismic sources, and the level of seismicity of the investigated area. Theoretical accelerations are computed by the modal summation technique (Panza, 1985; Florsch et al., 1991). The use of synthetic seismograms allows us to estimate, in a realistic way, the seismic hazard, also in those areas for which scarce (or none) historical or instrumental information is available. It is also possible to simulate quite easily different kinds of source mechanisms, to consider different structural models, and to compare the relative results in order to evaluate the influence of each parameter. To reduce the amount of computations, the seismic sources have been grouped in homogeneous seismogenic areas, and for each group the representative focal mechanism has

[1]Authors listed in alphabetical order.

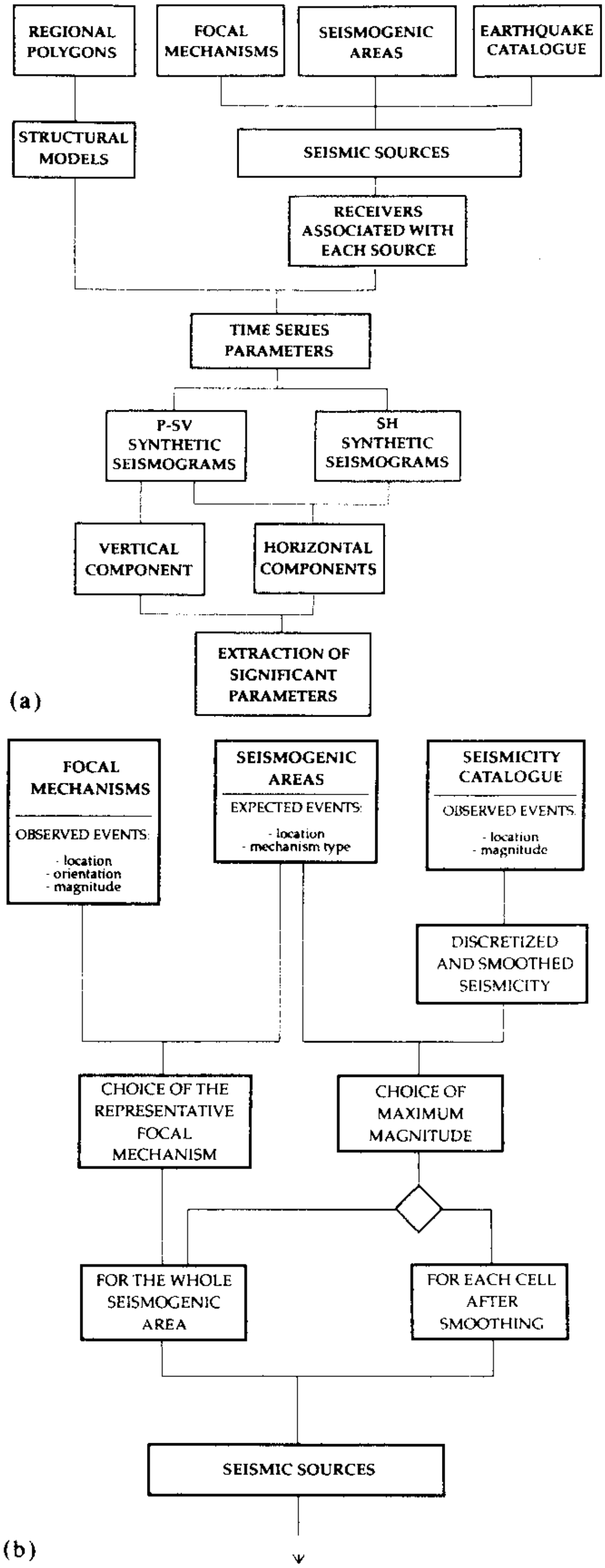


Fig. 1. (a) Flow-chart of the procedure. (b) Detail concerning the definition of seismic sources.

been kept constant. The seismic moment associated with each source is determined from the analysis of the maximum magnitude observed in the epicentral area in the past.

One way of representing the result of the procedure is to analyse the synthetic seismograms and to map the distribution of PGA over the investigated territory. The synthetic signals used for the prediction of the accelerations can be conveniently used as input data for more detailed zoning, based on the 2-D modelling of wave propagation (Fäh et al., 1990; Iodice et al., 1992). In this way, also the local soil effects can be taken into account.

The flow-chart of the procedure is shown in Fig. 1. In the following text, references to the flow chart are written in *italics*.

## Data

To compute the synthetic seismograms, the structures containing the source and the receivers must be defined, as well as the source characteristics. On the basis of the geologic characteristics, the Italian territory has been divided into 16 *polygons* (Fig. 2). Then a flat, layered *structural model* has been associated with each polygon. The different layers are described by their thickness, density, P- and S-wave velocities, and attenuation. The layering has been defined after an extensive bibliographic research, taking into account available DSS data (e.g. Schütte, 1978; Italian Explosion Seismology Group and Institute of Geophysics ETH, 1981; Nicolich, 1981; Bottari et al., 1982; Miller et al., 1982; Kern and Schenk, 1985; Scarascia and Pellis, 1985; Nicolich, 1989; Nicolas et al., 1990) and indirectly relevant data (e.g. Woollard, 1975).

The definition of the *seismic sources* has required the analysis of several data sets. To limit the spatial distribution of sources, we have used the 57 *seismogenic areas* (see Fig. 3) defined by the GNDT (1992) on the basis of seismological data and seismotectonic observations (e.g. Patacca et al., 1993).

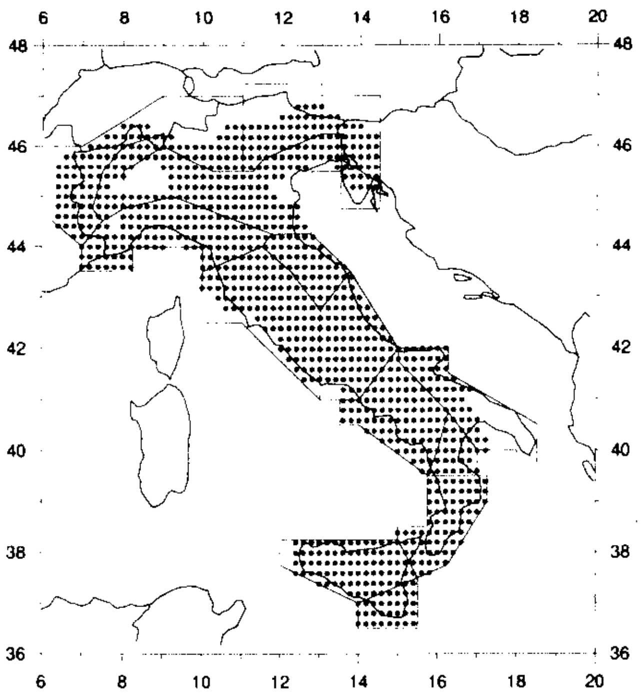


Fig. 2. Regional polygons associated with different structural models. The grid of dots represent the location of the receivers where synthetic seismograms have been computed.

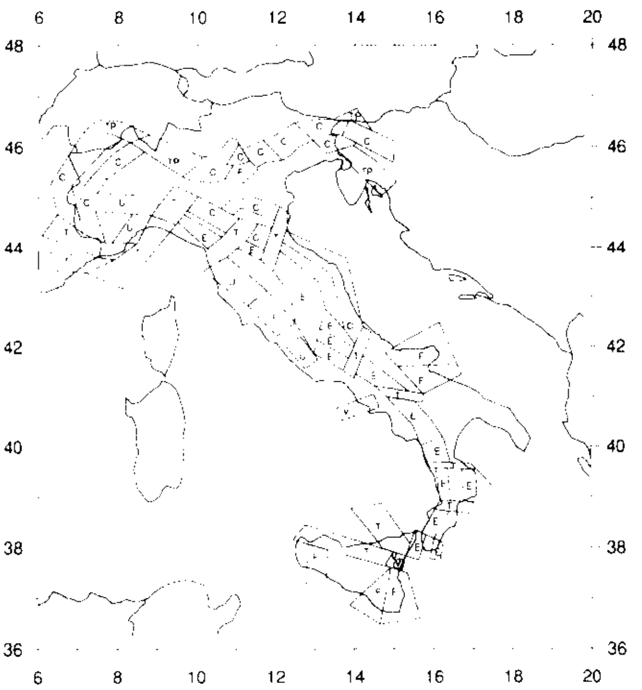


Fig. 3. Seismogenic zones defined by GNDT (1992). $C$=compressional areas; $E$=extensional areas; $F$=areas of fracture in foreland zones; $T$=transition areas; $TP$=areas of transpression; $U$=uncertain areas; $V$=volcanic areas.

For the definition of the source mechanisms, 305 fault-plane solutions, distributed over the whole territory, have been grouped in a database (Suhadolc, 1990; Suhadolc et al., 1992). The computer file contains a standard definition of the *focal mechanisms*, both as a function of strike, dip and rake of the nodal planes and as a function of the direction of compressional, tensional and null axes.

For the analysis of seismicity, an *earthquake catalogue* (PFGING) has been prepared, merging the data from the PFG (1985) catalogue, for the period 1000–1979, with the data from ING (1980–1991) bulletins, for the period 1980–1991. The original catalogues have been corrected for some obvious mistakes, like the presence of double or multiple events, time disorder and evident errors in the focal depths. Furthermore, only main shocks shallower than 50 km have been considered, removing aftershocks according to the algorithm suggested by Keilis-Borok et al. (1980).

We have considered only earthquakes that occurred within the PFG polygon (PFG, 1985). Therefore, the seismicity might be underestimated near political borders, and this could also have influenced the results (PGA distribution) in the regions close to these boundaries.

## Computations

To derive the distribution of the maximum observed magnitude over the territory, the image of the seismicity given by the earthquake catalogue has been smoothed. At first, the area has been subdivided into $0.2°\times0.2°$ cells. Each cell has been assigned the magnitude value of the most energetic event that occurred within it. The smoothing obtained through this discretization, however, was not found to be satisfactory, because not each cell does contain a statistically meaningful number of events. Therefore, the maximum magnitude to be associated with each cell has been searched for also in the cell surroundings, through the application of a centred smoothing window. More details about the discretization and smoothing of seismicity are given in Appendix 1.

For the definition of the seismic sources that are used to generate the synthetic seismograms, only the cells located within a seismogenic area are retained. The map shown in Fig. 4 is the result of the application of this method to the PFGING earthquake catalogue.

A double-couple point source is then placed in the centre of each cell. The orientation of the double couple associated with each source is obtained from the database of the fault-plane solutions. For each seismogenic area, a representative focal mechanism is selected through an automatic procedure. As a first simple hypothesis, the tensor elements of these mechanisms have been defined as the arithmetic average of the tensor elements of the available

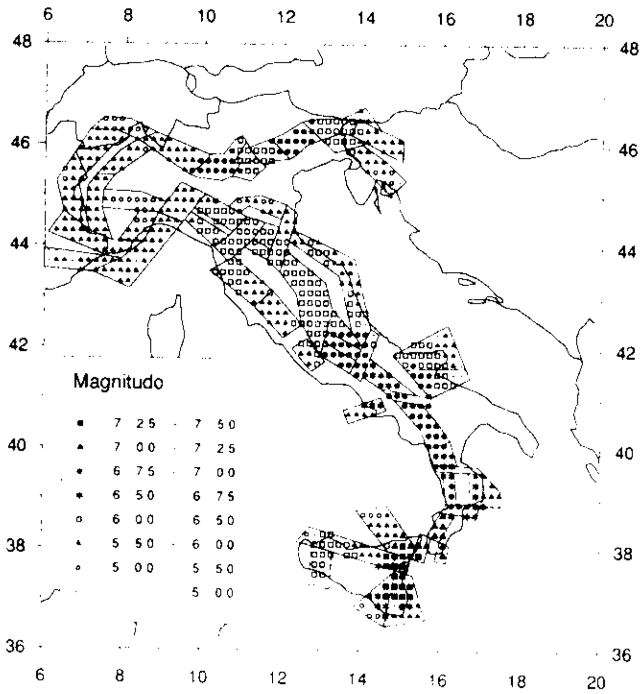


Fig. 4. Smoothed magnitude distribution for the cells belonging to the seismogenic zones shown in Fig. 3.

TABLE 1

The moment–magnitude relation

| Magnitude | $M_{0\,(1\,Hz)}$ (N·m) |
|---|---|
| 8.00≥M>7.75 | $4.00\times10^{18}$ |
| 7.75≥M>7.50 | $2.50\times10^{18}$ |
| 7.50≥M>7.25 | $1.60\times10^{18}$ |
| 7.25≥M>7.00 | $1.25\times10^{18}$ |
| 7.00≥M>6.75 | $5.00\times10^{17}$ |
| 6.75≥M>6.50 | $3.15\times10^{17}$ |
| 6.50≥M>6.00 | $1.60\times10^{17}$ |
| 6.00≥M>5.50 | $4.00\times10^{16}$ |
| 5.50≥M>5.00 | $1.40\times10^{16}$ |
| 5.00≥M | $4.00\times10^{15}$ |

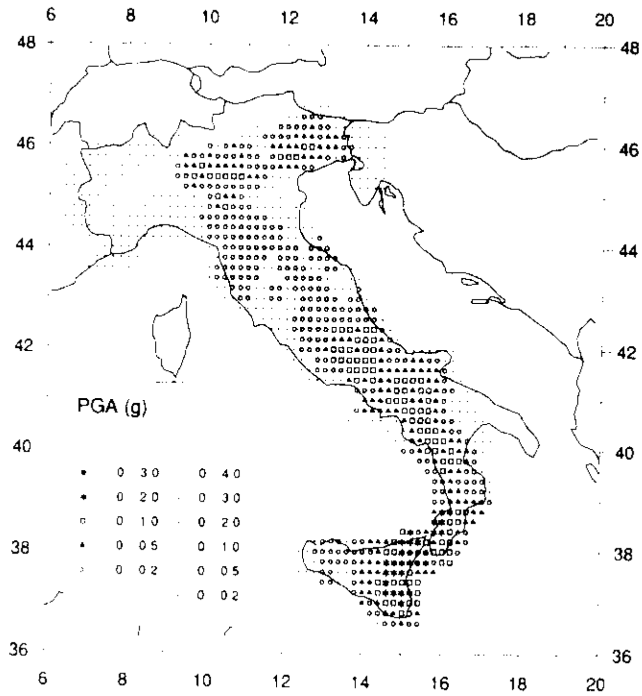


Fig. 5. Estimated distribution of horizontal peak ground acceleration.

TABLE 2

The intensity–acceleration relation

| Intensity | Acceleration[1] | |
|---|---|---|
| | $cm\cdot s^{-2}$ | $g$ |
| XII | 492.5 | 0.50 |
| XI | 370.9 | 0.38 |
| X | 284.4 | 0.29 |
| IX | 222.1 | 0.23 |
| VIII | 176.5 | 0.18 |
| VII | 142.9 | 0.15 |
| VI | 117.7 | 0.12 |
| V | 98.7 | 0.10 |
| IV | 84.3 | 0.09 |

[1]Estimates from Boschi et al., 1969.

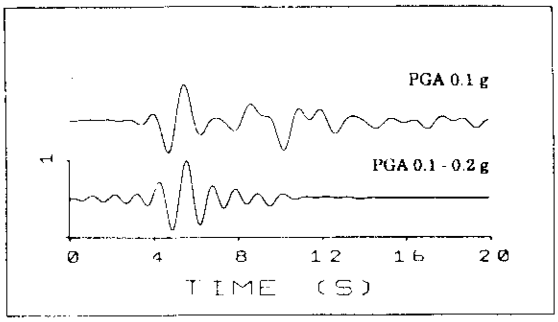


Fig. 6. Comparison between NS acceleration recorded at the station of Sturno during the Irpinia earthquake of 23 November 1980 (above) and one synthetic signal computed for that area (below) on the basis of the procedure described in this work. Accelerations have been low-pass filtered with a cut-off frequency of 1 Hz.

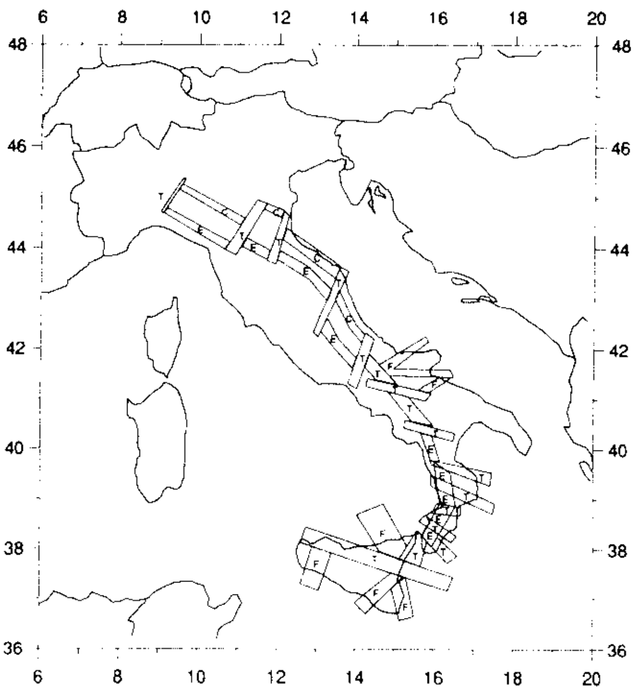


Fig. 7. Seismogenic zones given by GNDT as a preliminary result in the seismogenic zonation of the Italian territory. This model, that we refer to as Model $A$, must be compared with the one shown in Fig. 3. $C$=compressional areas; $E$=extensional areas; $F$=areas of fracture in foreland zones; $T$=transition areas.

mechanisms. This procedure appears to be reasonable when the mechanisms are not too different to average, and this condition has been checked for each seismogenic area.

Once the structures and the sources have been defined, *receivers* are placed on a grid

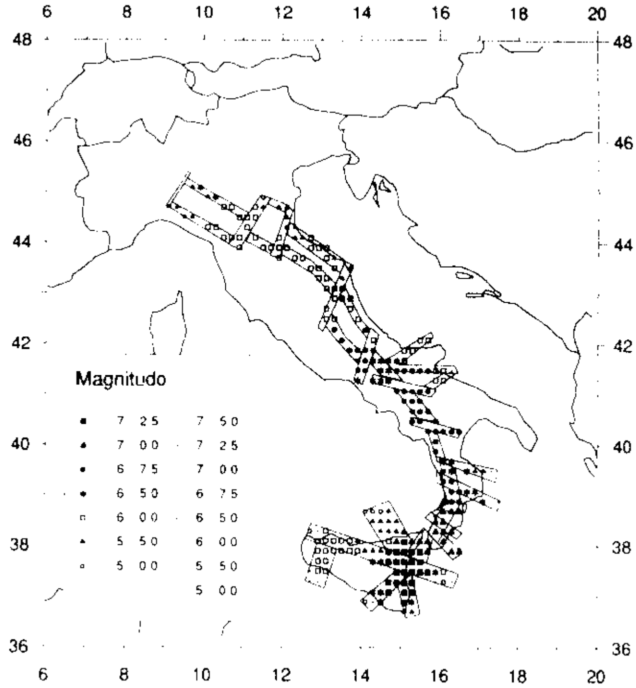


Fig. 8. Smoothed magnitude distribution for the cells belonging to the seismogenic zones shown in Fig. 7.

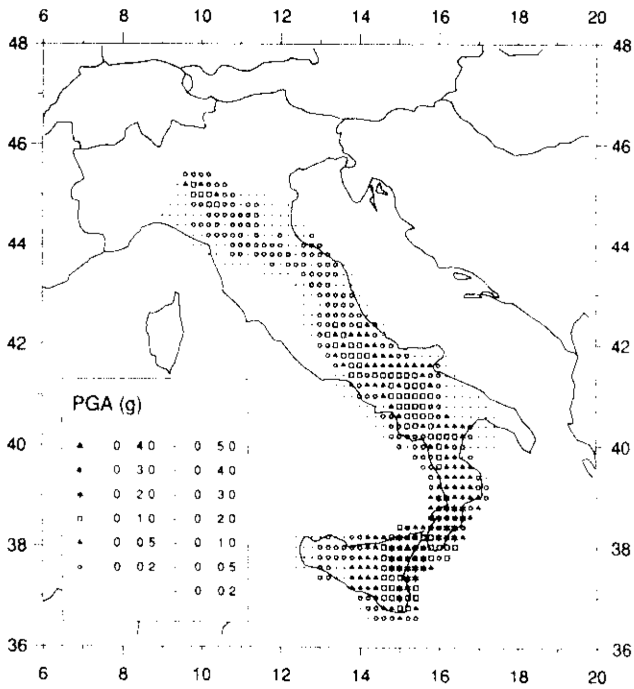


Fig. 9. Estimated distribution of the horizontal peak ground acceleration obtained using the seismogenic zones of Fig. 7. For a stability test it should be compared with Fig. 5.

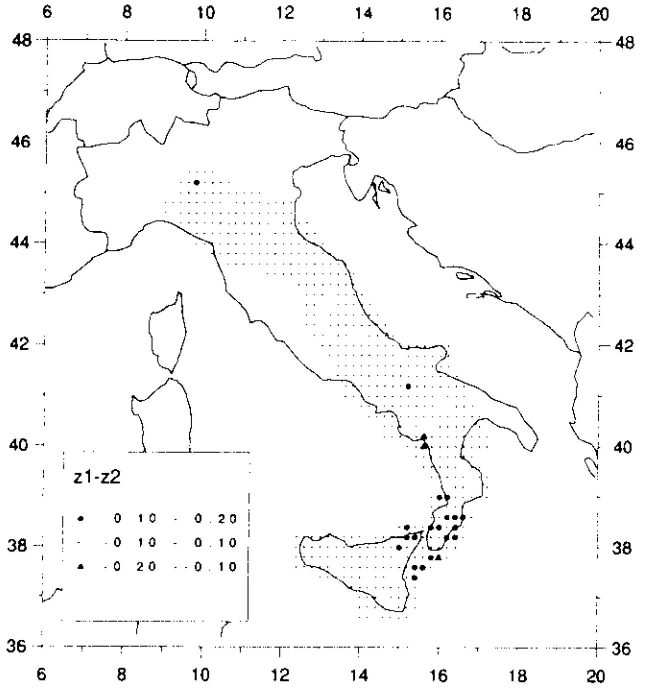


Fig. 10. Map of the relevant discrepancies between the PGA values shown in Figs. 5 and 9.

(0.2° × 0.2°) covering the whole territory and synthetic seismograms are efficiently computed by the modal summation technique (Panza, 1985; Florsch et al., 1991). In this first example, the synthetic signals are computed for an upper frequency content of 1 Hz, and the point-source approximation is still acceptable. This is fully justified by practical considerations, because, for instance, several-story buildings have a peak response in the frequency range below 1 Hz (e.g. Manos and Demosthenous, 1992). When shorter periods are considered, it will be no longer possible to neglect the finite dimensions of the faults and the rupturing process at the source.

To reduce the number of the computed seismograms, the source–receiver distance is kept below an upper threshold, which is taken to be a function of the magnitude associated with the source. The maximum source–receiver distance has been set equal to 25, 50, and 90 km for $M < 6$, $6 \leq M < 7$ and $M \geq 7$, respectively. All seismograms have been computed for a constant hypocentral depth (10 km), but it is also possible to assign to each source an average depth determined from the analysis of catalogues of past seismicity. The reason to keep the hypocentral depth fixed and shallow is to be found in the large errors affecting the hypocentral depth estimates in the PFGING catalogue and in the fact that strong ground motion is mainly controlled by shallow sources (e.g. Vaccari et al., 1990).

*P–SV* (radial and vertical components) and *SH* (transverse component) *synthetic seismograms* are originally computed for a seismic moment of $1 \times 10^{-7}$ N·m. The amplitudes are then properly scaled according to the (smoothed) magnitude associated with the cell of the source. For the moment–magnitude relation, we have chosen the one given by Boore (1987). To obtain the values given in Table 1, which are valid for the frequency of 1 Hz, we have used the scaling law proposed by Gusev (1983). The idea of a constant magnitude within each seismogenic area (choosing the maximum available value) has been discarded because, for the larger seismogenic areas, it leads to an over-estimation of the seismicity.

At each receiver, the horizontal components are first rotated to a reference system common to the whole territory (N–S- and E–W-directions) and then the vector sum is computed. For the *significant parameters* representative of the strong ground motion we have, for the moment, focused our attention on the peak ground acceleration values (PGA). As we compute the complete time series, we are not limited to this choice, and it is also possible to consider other parameters, like Arias (1970) intensity or other integral quantities that can be of interest in seismic engineering. Because recordings of many different sources are associated to each receiver, but one single value is to be plotted on a map (Fig. 5), only the maximum value of the analysed parameter is considered.

## Discussion and conclusions

The intensity–acceleration relation proposed by Boschi et al. (1969) has been used to

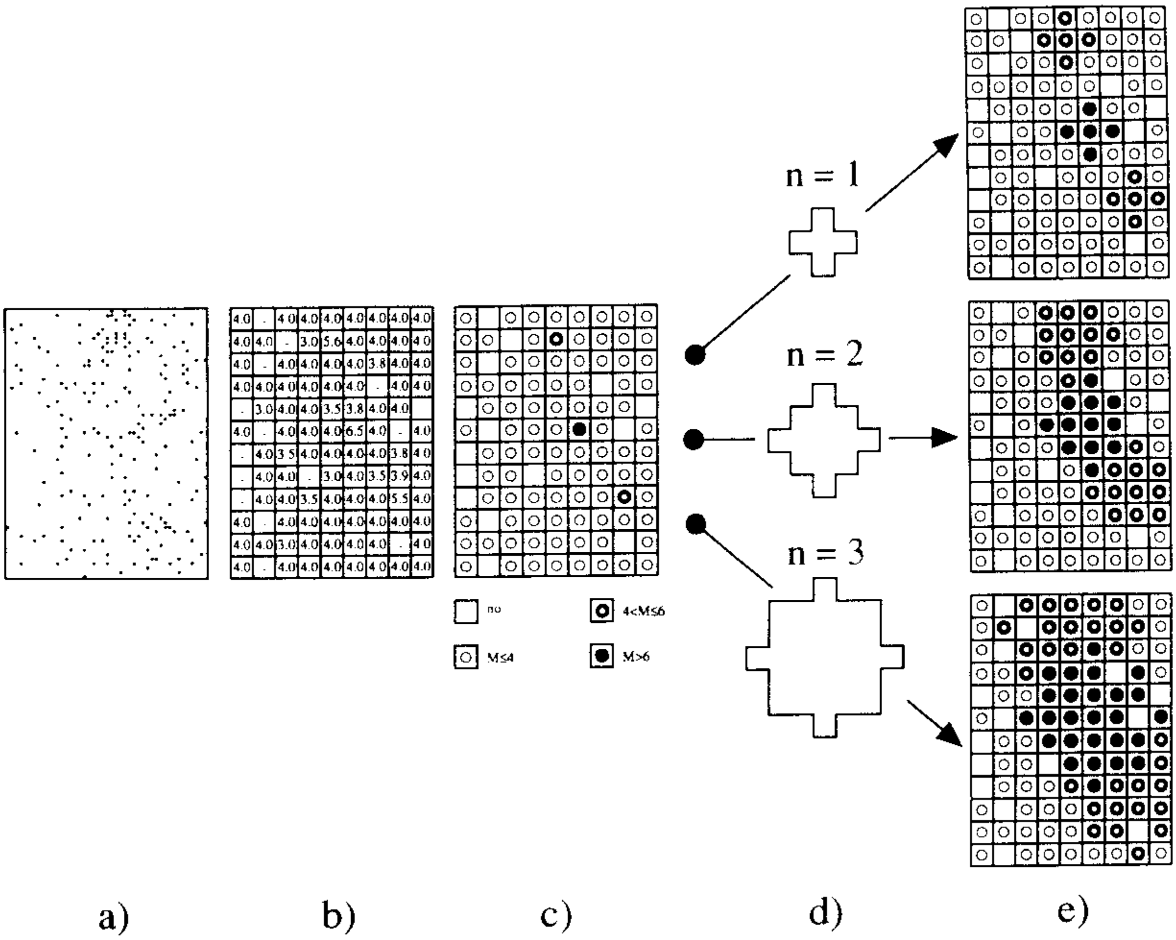


Fig. 11. Discretization and smoothing of seismicity. **a**=distribution of epicentres; **b**=definition of cells and choice of maximum magnitude; **c**=graphic representation of **b**; **d**=smoothing windows of radius $n=1$, $n=2$, $n=3$; **e**=smoothed distribution of magnitude.

compare the results of Fig. 5 with the historical data, for which only macroseismic intensity estimates exist (see Table 2). We have checked that the computed PGA values are compatible with the above mentioned relation.

A more quantitative check has been made using the observed accelerograms recorded during the Irpinia earthquake on 23 November 1980. It is well known that the source rupturing process of that event is very complex (e.g. Bernard and Zollo, 1989), and the dimension of the source has been estimated to be of the order of several tens of kilometres. Nevertheless, it seems that the signal recorded at the station of Sturno is mostly due to a single sub-event that occurred rather close to the station itself, while the energy contributions coming from other regions of the source seem irrelevant (Vaccari et al., 1990). We have low-pass filtered the NS accelerogram recorded at Sturno with a cut-off frequency at 1 Hz to compare it with one of the computed signals for the Irpinia region (Fig. 6). The early phases and the PGA of the two time series are in very good agreement. The late part of the observed recording is more complicated and this is related to the complexity of the source, which has been neglected in the computation of the synthetic signal.

The definition of seismogenic structures of the Italian territory, given by GNDT (1982), is the final result of a fruitful cooperation be-

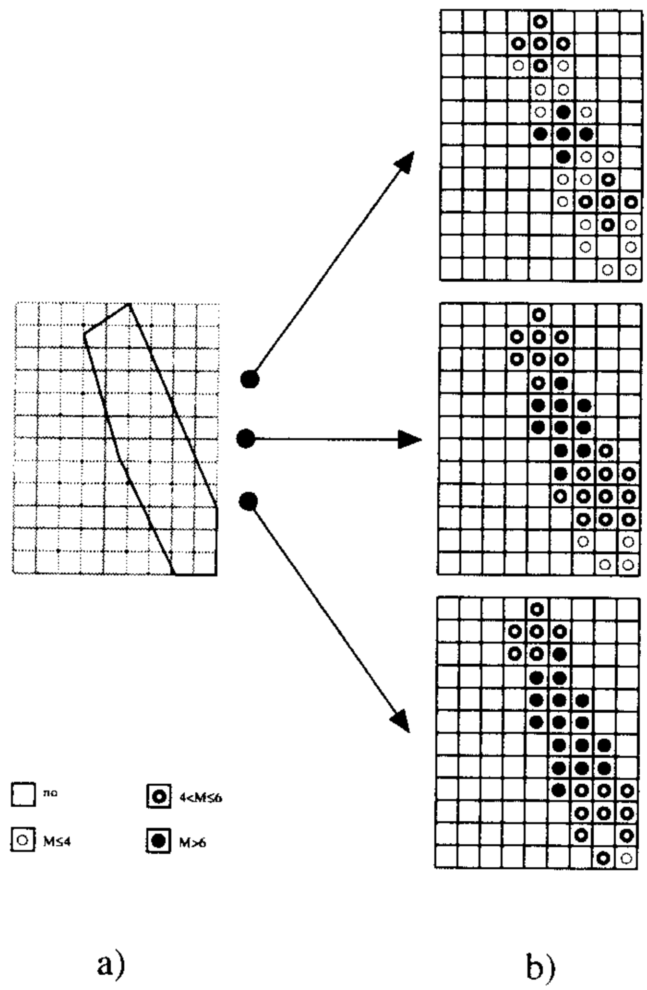


Fig. 12. Hypothetical seismogenic zone (a) and its intersection with the example data of Fig. 11e (b).

tween structural geologists and seismologists from all over Italy. In developing the project, several proposals have been made and some provisional hypothesis have been considered. Taking advantage of those existing alternatives, it has been possible to test the stability of our results, namely the PGA distribution, versus the distribution of seismogenic structures. Model *A* is one intermediate result of the GNDT project, as it does not include the Alpine Arc (Fig. 7) and can be compared with the more recent, presently accepted, model of Fig. 3, which was used to compute the PGA distribution shown in Fig. 5. In the common regions, some relevant differences can be evidenced in the Lazio and Toscana regions, as well as in the Gargano peninsula. Furthermore, in the more recent model, the Calabrian Arc is characterised by a much more simplified zonation. The smoothed magnitudes associated with the seismogenic zones of Model *A* are given in Fig. 8. Figure 9 shows the PGA distribution obtained using Model *A* and should be compared with Fig. 5. It can be noticed that in the common areas the regions where maximum accelerations are expected to occur are almost the same, and also the PGA values do not differ too much. Relevant discrepancies, between 0.1 and 0.2 *g*, can only be found in relation with the Calabrian Arc (see Fig. 10) where, due to the larger spatial extension of seismogenic areas, Model *A* implies PGA values also in the class 0.40–0.50 *g*.

This comparison shows one important advantage of the procedure, namely the possibility of easily testing the influence of any parameter that is used as input data. An important stability test will be performed as soon as the revised earthquake catalogue by GNDT will be available. Stability tests are currently being performed analysing the catalogues in different periods of time.

## Appendix 1. Discretization and smoothing of seismicity

The first problem to tackle in the definition of seismic sources is the handling of seismicity data. What is needed for the procedure described in this paper and will be used in the computation of synthetic seismograms is a distribution over the territory of the maximum magnitude. Data available from earthquake catalogues are, on the contrary, discrete and punctual. Furthermore, a 2-dimensional distribution requires a large amount of samples to be well determined, but earthquake catalogues are both incomplete and affected by errors, so a smoothed distribution is preferable (Panza et al., 1990). A smooth distribution can be misleading in the fact that it assignes some values also to areas where data are absent. To

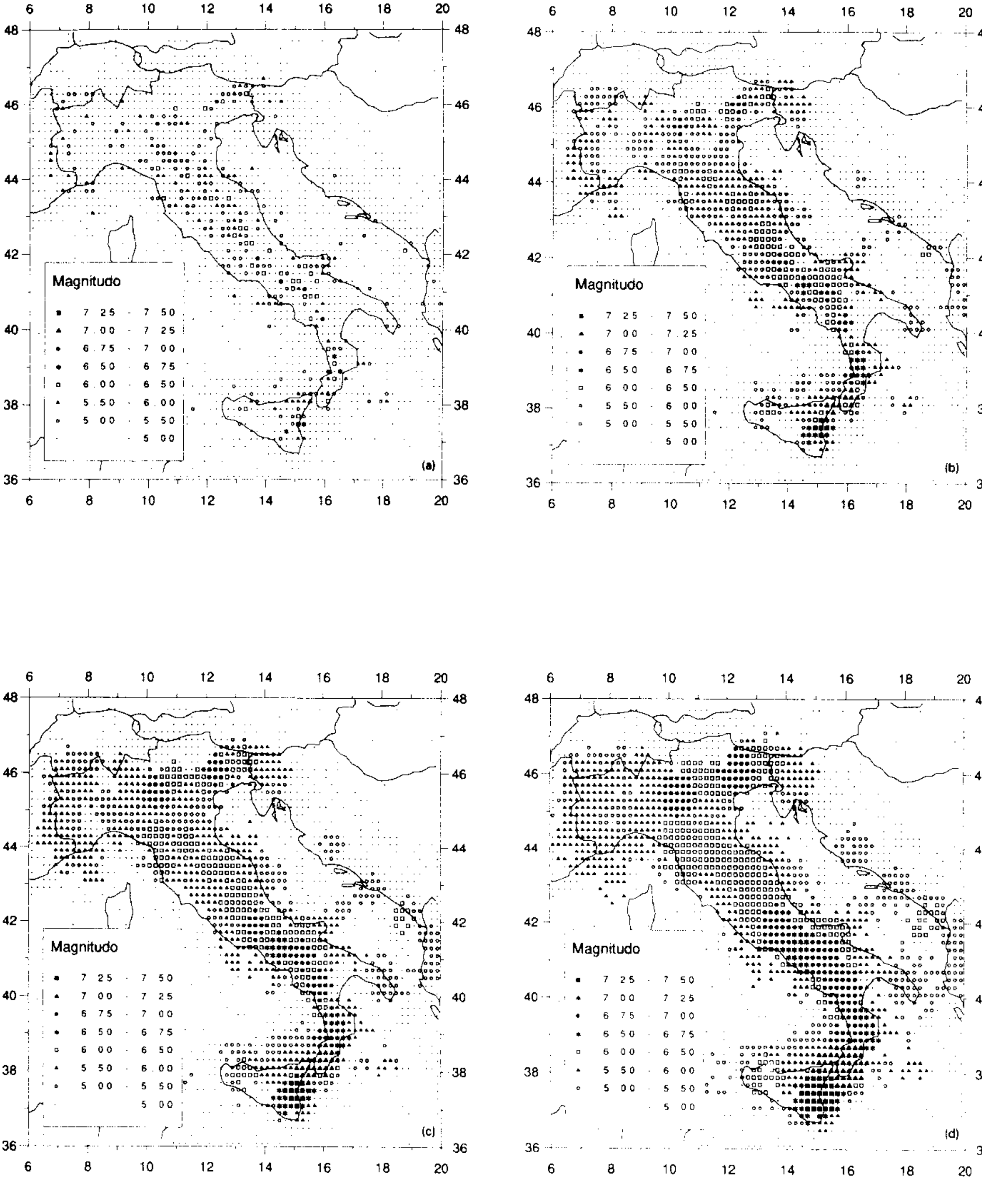


Fig. 13. Magnitude distribution after the application of discretization and smoothing to the seismicity data given in catalogue PFGING after aftershock removal. Radius of smoothing window: (a) $n=0$; (b) $n=1$; (c) $n=2$; (d) $n=3$.

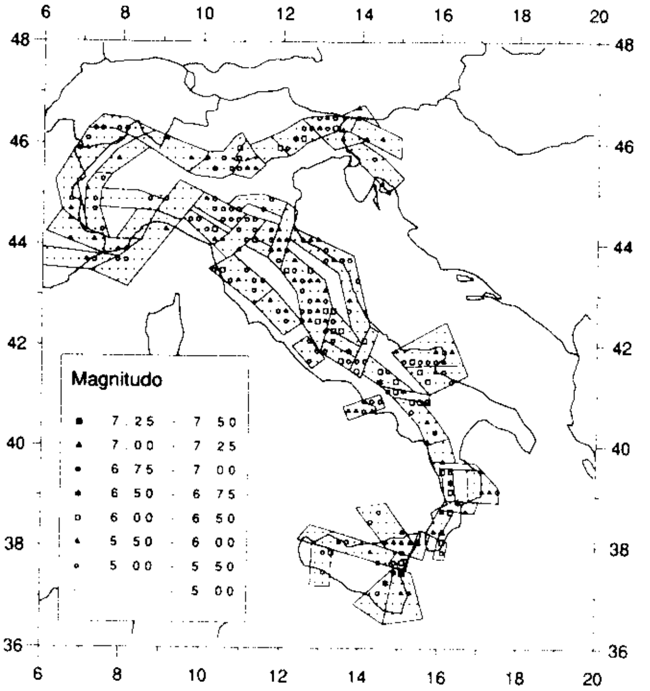


Fig. 14. Intersection between the seismogenic zones of Fig. 3 and the seismicity image of Fig. 13a.

avoid this drawback, we have decided to represent seismicity by cells. The size of the cells can be related with errors in the location of earthquakes. On the basis of experience (Suhadolc, 1990) the dimensions of $0.2° \times 0.2°$ have been chosen, even if for historical earthquakes such a resolution could be considered optimistic.

The smoothing procedure is shown in Fig. 11. At first, the punctual distribution of epicentres given in Fig. 11a is discretised into cells (Fig. 11b) and the maximum magnitude of the events pertinent to each cell is retained. In case the earthquake catalogue contains different estimates of the magnitude (e.g. magnitude computed from body waves, from surface waves, from macroseismic intensity), the maximum between them is considered. It is then convenient to represent the data graphically, where symbols are associated with magnitude ranges (Fig. 11c).

In most cases, the smoothing obtained by just considering cells is not enough, because from a statistical point of view single cells do not contain a meaningful number of events. A centered smoothing window is then considered. Earthquake magnitudes are analysed not only in the central cell, but also in neighboring ones. The maximum value of magnitude found in the window is assigned to the central cell only if the cell itself contains a minimum number of earthquakes. For this purpose, several thresholds have been tested (one to four earthquakes): the increase in the threshold is related to a more stable representation of seismicity, because sporadic events, that could be the result of mislocations or singularities of the seismic regime, are eliminated. We have noticed that only areas with very low seismicity, not included in the seismogenic areas shown in Fig. 3, are sensible to modifications of the threshold in the range 1 to 3. Therefore, taking into consideration only the seismogenic areas, stability is already ensured if the lower threshold (one earthquake) is selected.

Three possible smoothing windows are shown in Fig. 11d. Their "radius" is expressed in terms of number of cells, $n$. In the example, the values $n=1$, $n=2$ and $n=3$ are considered. By applying those windows to the distribution of Fig. 11c, the results of Fig. 11e are obtained. At a first glance, it appears that the distribution of maximum magnitude given by the window with $n=3$ is quite exaggerated with respect to the starting data of Fig. 11c, but its intersection with an hypothetic seismogenic area (shown in Fig. 12a) gives quite reasonable results (Fig. 12b).

The smoothing algorithm has been applied to the catalogue of main shocks for the Italian territory. Windows of radius $n=0$ (which corresponds to considering just the central cell), $n=1$, $n=2$ and $n=3$ have been used, obtaining the results shown in Fig. 13a–d, respectively. The intersection of the map of Fig. 13d with the seismogenic areas of Fig. 3, defined by GNDT (1992), is already shown in Fig. 4. The radius $n=3$ has been selected because a good degree of homogeneity in the distribution of magnitude seems appropriate within each seismogenic area. This condition is not verified if the smoothing is not applied (see Fig. 14).

## Acknowledgements

This study has been made possible by the CNR contracts 90.02382.CT15, 90.01026.PF54. We would like to thank ENEA for allowing us the use of the IBM3090E computer at the ENEA INFO BOL Computer Center. This research has been carried out in the framework of the activities of the ILP Task Group II.4.

## References

Arias, A., 1970. A measure of earthquake intensity. In: R. Hansen (Editor), Seismic Design for Nuclear Power Plants. Cambridge, MA, pp. 438–483.

Bernard, P. and Zollo, A., 1989. The Irpinia (Italy) 1980 earthquake: detailed analysis of a complex normal faulting. J. Geophys. Res., 94: 1631–1647.

Boore, D.M., 1987. The prediction of strong ground motion. In: M.Ö. Erdik and M.N. Toksöz (Editors), Strong Ground Motion Seismology. Reidel, Dordrecht, pp. 109–141.

Boschi, E., Caputo, M. and Panza, G.F., 1969. Stability of seismic activity in Italy with special reference to Garfagnana, Mugello and Forlivese. Rapp. CNEN RT/ING(69)24, pp. 1–24.

Bottari, A., Caccamo, D., Carapezza, E., Cosentino, M., Cosentino, P., Federico, B., Fradella, P., Hoang Trong, P., Lo Giudice, E., Lombardo, G., Neri, G. and Patanè, G., 1982. Crustal regional travel times of P and S waves in Sicily. CNR, Roma. Atti 2° Conv. GNGTS, pp. 605–614.

Fäh, D., Suhadolc, P. and Panza, G.F., 1990. Estimation of strong ground motion in laterally heterogenenous media: modal summation–finite differences. Proc. 9th Eur. Conf. Earthquake Eng., Sept. 11–16, 1990, Moscow. 4A, pp. 100–109.

Florsch, N., Fäh, D., Suhadolc, P. and Panza, G.F., 1991. Complete synthetic seismograms for high-frequency multimode Love waves. Pure Appl. Geophys., 136: 529–560.

GNDT, 1992. Convegno Nazionale sul Modello Sismotettonico d'Italia. Milano, 25–26 May.

Gusev, A.A., 1983. Descriptive statistical model of earthquake source radiation and its application to an estimation of short period strong motion. Geophys. J.R. Astron. Soc., 74: 787–800.

ING, 1980–1991. Istituto Nazionale di Geofisica. Seismological reports. ING, Roma.

Iodice, C., Fäh, D., Suhadolc, P. and Panza, G.F., 1992. Un metodo generale per la zonazione sismica rapida ed accurata di grandi metropoli: applicazione alla città di Roma. Rend. Fis. Accad. Lincei, 3: 195–217.

Italian Explosion Seismology Group and Institute of Geophysics, ETH, Zürich, 1981. Crust and upper mantle structures in the Southern Alps from deep seismic sounding profiles (1977, 1978) and surface waves dispersion analysis. Boll. Geofis. Teor. Appl., 23: 297–330.

Keilis-Borok, V.I., Knopoff, L., Rotwain, I.M. and Sidorenko, T.M., 1980. Bursts of seismicity as long-term precursors of strong earthquakes. J. Geophys. Res., 85: 803–812.

Kern, H. and Schenk, V., 1985. Elastic wave velocities from a lower crustal section in Southern Calabria (Italy). Phys. Earth Planet. Inter., 40: 147–160.

Manos, G.C. and Demosthenous, M., 1992. Design of R.C. structures according to the Greek Seismic Code Provisions. Bull. IISEE, 26: 559–578.

Miller, H., Mueller, St. and Perrier, G., 1982. Structure and dynamics of the Alps: a geophysical inventory. In: H. Berkhemer and U. Hsü (Editors) Alpine–Mediterranean Geodynamics. Am. Geophys. Union, Geophys. Ser., 7, pp. 175–203.

Nicolas, A., Polino, R., Hirn, A., Nicolich, R. and ECORS–CROP Working Group, 1990. ECORS–CROP traverse and deep structures of the Western Alps: a synthesis. In: R. Roure, P. Heitzman and R. Polino (Editors), Deep Structure of the Alps. Mém. Soc. Geol. Fr. Ital. Suisse, pp. 15–27.

Nicolich, R., 1981. Il profilo Latina–Pescara e le registrazioni mediante OBS nel Mar Tirreno. CNR, Roma. Atti 1° Conv. GNGTS, pp. 621–634.

Nicolich, R., 1989. Crustal structures from seismic studies in the frame of the European Geotraverse (Southern Segment) and CROP projects. Atti Conv. Lincei, 80: 41–61.

Panza, G. F., 1985. Synthetic seismograms: The Rayleigh waves modal summation. J. Geophys., 58: 125–145.

Panza, G. F., Prozorov, A. and Suhadolc, P., 1990. Is there a correlation between lithosphere structure and statistical properties of seismicity? In: R. Cassinis and G.F. Panza (Editors), The Structure of the Alpine–Mediterranean area: Contribution of Geophysical Methods. Terra Nova, 2: 585–595.

Patacca, E., Sartori, R. and Scandone, P., 1992. Tyrrhenian basin and Apenninic arcs: kinematic relations since late Tortonian times. Mem. Soc. Geol. Ital., in press.

PFG, 1985. Catalogo dei terremoti italiani dall'anno 1000 al 1980 [Edited by D. Postpischl]. CNR, Prog. Final. Geodin., Roma, pp. 1–239.

Scarascia, S. and Pellis, G., 1985. Crustal structure of the Northern Apennine. Part A—The upper crust. In: D.A. Galson and St. Mueller (Editors), Proc. 2nd Workshop on the European Geotraverse (EGT) Project, The Southern Segment. European Science Fundation, Strasbourg, pp. 137–142.

Schütte, K.G., 1978. Crustal structure of Southern Italy. In: H. Closs, D. Roeder and K. Schmidt (Editors), Alps, Apennines and Hellenides. IUGG, 38: 374–388.

Suhadolc, P., 1990. Fault-plane solutions and seismicity around the EGT southern segment. In: R. Freeman and St. Mueller (Editors), Proc. 6th Workshop on the European Geotraverse (EGT), Data compilations and synoptic interpretation. European Science Foundation, Strasbourg, pp. 371–382.

Suhadolc, P., Panza, G.F., Marson, I., Costa, G. and Vaccari, F., 1992. Analisi della sismicità e meccanismi focali nell'area italiana. Atti Conv. Gruppo Naz. Difesa Terremoti, Pisa, 1990, 1: 157–168.

Vaccari, F., Suhadolc, P. and Panza, G.F., 1990. Irpinia, Italy, 1980 earthquake: waveform modelling of strong motion data. Geophys. J. Int., 101: 631–647.

Woollard, G.P., 1975. Regional changes in gravity and their relation to crustal parameters. Bur. Grav. Int. Bull. Inf., 36: 106–110.

ELSEVIER

Tectonophysics 258 (1996) 263–274

TECTONOPHYSICS

# Estimates of 1 Hz maximum acceleration in Bulgaria for seismic risk reduction purposes

I.M. Orozova-Stanishkova *, G. Costa, F. Vaccari, P. Suhadolc

*Dipartimento Scienze della Terra, Università degli Studi di Trieste, via E. Weiss 1, 34127 Trieste, Italy*

Received 17 May 1995; accepted 30 November 1995

**Abstract**

The regional seismic hazard in Bulgaria is assessed using a deterministic approach, which computes synthetic seismograms at a set of grid points. The input for this computation is represented by available source and structural models. A set of simplified structural models is proposed for Bulgaria and assigned to a number of regional polygons. The set of seismic sources are parametrized using the knowledge about the focal mechanisms, the seismogenic areas and the regional seismicity. A map of the maximum ground acceleration (AMAX) is chosen to represent the shakeability and the seismic hazard. The most dangerous area of the country is confirmed as southwestern Bulgaria.

## 1. Introduction

Bulgaria is a country with a high level of seismic hazard (Bonchev et al., 1982; Reisner, 1988; Orozova-Stanishkova and Slejko, 1994). The seismic history mentions four large earthquakes ($M_s \geq 7$) during the last century on the territory of the country. The strongest events which occurred over the Bulgarian territory are given in Table 1.

Various studies have been performed in the past to evaluate the shakeability (Bonchev et al., 1982) and the probability of strong ($M > 6.8$) earthquakes (Reisner, 1988) in Bulgaria on the basis of a global analysis of geological, geophysical and seismological data. Recently, Orozova-Stanishkova and Slejko (1994) have calculated the seismic hazard of Bulgaria using different probabilistic approaches (e.g. Gumbel, 1966; Cornell, 1968), and seismogenic zones together with a simplified tectonic scheme.

A deterministic approach to estimate the Maximum Ground Acceleration (AMAX) has been developed by Costa et al. (1993). This procedure, starting from the available information on the Earth structure parameters, the seismic sources and the level of the seismicity of the investigated area, computes synthetic seismograms. The use of synthetic seismograms allows to estimate, in a rather realistic way, the engineering parameters needed to assess the seismic hazard. Moreover, the approach allows to estimate these parameters also in those areas, where scarce (or none) historical or instrumental information is available. Because the method allows to simulate quite easily different kinds of source mechanisms, to consider different structural models etc., it is also possible to evaluate the influence of each parameter on the final result. One of the outcomes of

* Corresponding author. Fax: +39-40 575-519.


*SSDI* 0040-1951(95)00205-7

Table 1
Strongest earthquakes in Bulgaria

| Year | Place | Magnitude |
|---|---|---|
| 536 | NE Bulgaria | 7.5 |
| 542 | NE Bulgaria | 7.5 |
| 553 | NE Bulgaria | 7.5 |
| 1444 | NE Bulgaria | 7.5 |
| 1641 | S Bulgaria | 7.0 |
| 1750 | S Bulgaria | 7.5 |
| 1858 | Sofia | 6.5 |
| 1901 | Shabla | 7.2 |
| 1904 | Kresna | 7.8 |
| 1913 | Gorna Oryakhovitza | 7.0 |
| 1928 | Chirpan | 7.0 |
| 1986/Feb. | Strazhitza | 5.5 |
| 1986/Dec. | Strazhitza | 5.7 |

the procedure is a map showing the distribution of AMAX over the investigated territory.

The aim of the present study is to give a contribution to the seismic hazard studies for Bulgaria using the deterministic method, briefly described above, and to compare the obtained results with those arising from the probabilistic methods.

## 2. Input data

In order to compute synthetic seismograms, it is necessary to take into account source and propagation effects. Therefore, one has to assign the seismic source parameters and the structural model to the studied area. The flow-chart scheme of the method is given in Fig. 1. As it can be seen, the input data consist of four main sections: regional polygons, focal mechanisms, seismogenic areas and the earthquake catalogue. The regional polygons limit the area of validity of the structural model, whereas the focal mechanisms, the seismogenic areas and the earthquake catalogue are used in the characterization of the seismic sources. A brief description of the different inputs is given below.

The *regional polygons* are the surface delineations of different *structural models*. These models characterize different lithospheric properties of the studied area. They are defined within the regional polygons and are represented by a number of flat layers, to each of which the thickness, density, P-and S-waves velocities and their attenuation is assigned. The structural models determine the propagation effects and, therefore, influence the final results. In order to propose a suitable structural model it is necessary to consider the available geophysical and geological information for the investigated territory. In the present study the Bulgarian territory is divided into six regional polygons (Fig. 2), using the information about the tectonic and geologic characteristics (Bonchev et al., 1982), the thickness of the Earth's crust (Bonchev et al., 1982; Dachev and Volvovsky, 1985; Shanov and Kostadinov, 1992) together with some P-wave velocity models (Dotzev and Yunga, 1988; Sokerova and Velichkova, 1989; Stanishkova and Slejko, 1990). Eight flat layers have been proposed to define the crustal structure within each of the polygons. The parameters of the layers (depth of the layer top and P-wave velocity) are given in Table 2. The S-wave velocity is assigned to be equal to $Vp/1.7$. The quality factors and the parameters of the layers, when not available from the literature, were assumed to be equal to those given in Costa et al. (1993).

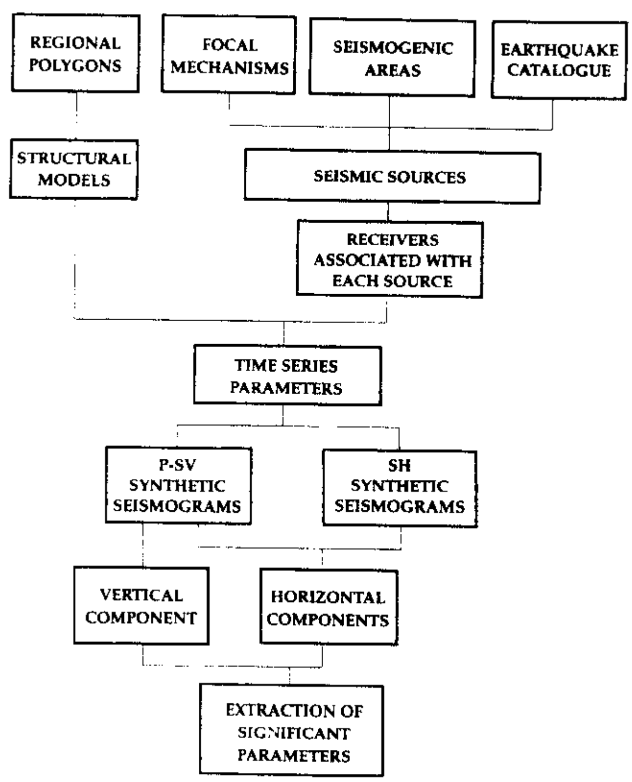


Fig. 1. Flow-chart scheme of the deterministic procedure in the estimate of maximum ground acceleration.

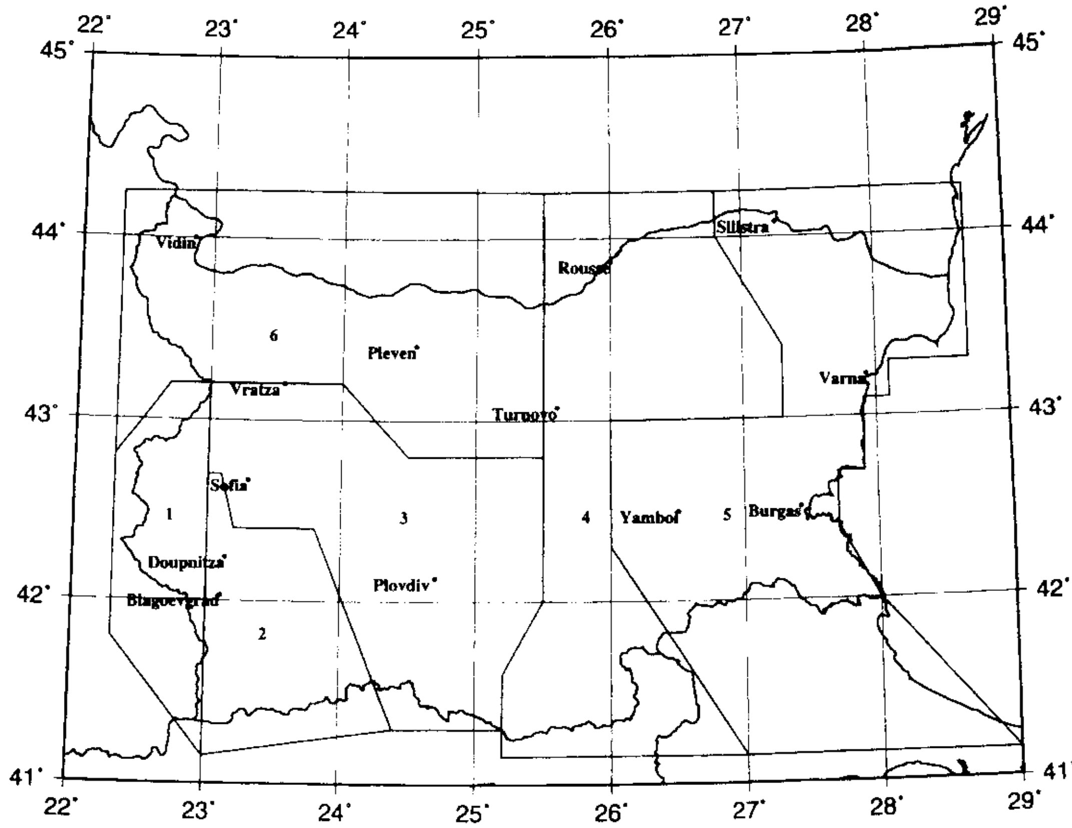


Fig. 2. Boundaries of the polygons in Bulgaria, to which regional structural models to be used in the calculations are assigned.

The used *focal mechanisms* are based on a number of published fault-plane solutions over the territory of Bulgaria (Dotzev and Yunga, 1988; Stanishkova and Slejko, 1991; Shanov and Georgiev, 1992; Shanov et al., 1992; Solakov and Simeonova, 1993). The computer file contains the parameters of about 170 focal mechanisms (mainly derived from Solakov and Simeonova, 1993), both as strike, dip and rake of the nodal planes, and as trend and plunge of the principal stress axes.

The *seismogenic areas* (or zones) are the final result of the seismic zoning of a certain territory. Each of them is characterized by a specific tectonic, geodynamic and seismic behaviour, which is assumed to be homogeneous within the zone. A large amount of geologic, tectonic and seismological information has to be analyzed in order to define these zones.

On the basis of the geologic, tectonic and seismicity evidences, Stanishkova and Slejko (1991) and

Table 2
Main layer parameters defining the structural model in each polygon

| | | | | | | | | | |
|---|---|---|---|---|---|---|---|---|---|
| | *Vp* (km/s) | 5.2 | 5.7 | 5.9 | 6.0 | 6.7 | 7.2 | 7.8 | 8.0 |
| | *Vs* (km/s) | 3.1 | 3.3 | 3.5 | 3.5 | 3.9 | 4.2 | 4.6 | 4.7 |
| Polygon number | Depth (km) | | | | | | | | |
| 1 | | 0 | 5 | 17 | 23 | 26 | 33 | 37 | 40 |
| 2 | | 0 | 5 | 18 | 25 | 28 | 37 | 42 | 45 |
| 3 | | 0 | 4 | 15 | 20 | 23 | 32 | 37 | 40 |
| 4 | | 0 | 3 | 12 | 17 | 20 | 27 | 31 | 33 |
| 5 | | 0 | 3 | 11 | 15 | 17 | 23 | 27 | 30 |
| 6 | | 0 | 4 | 15 | 20 | 22 | 28 | 31 | 34 |

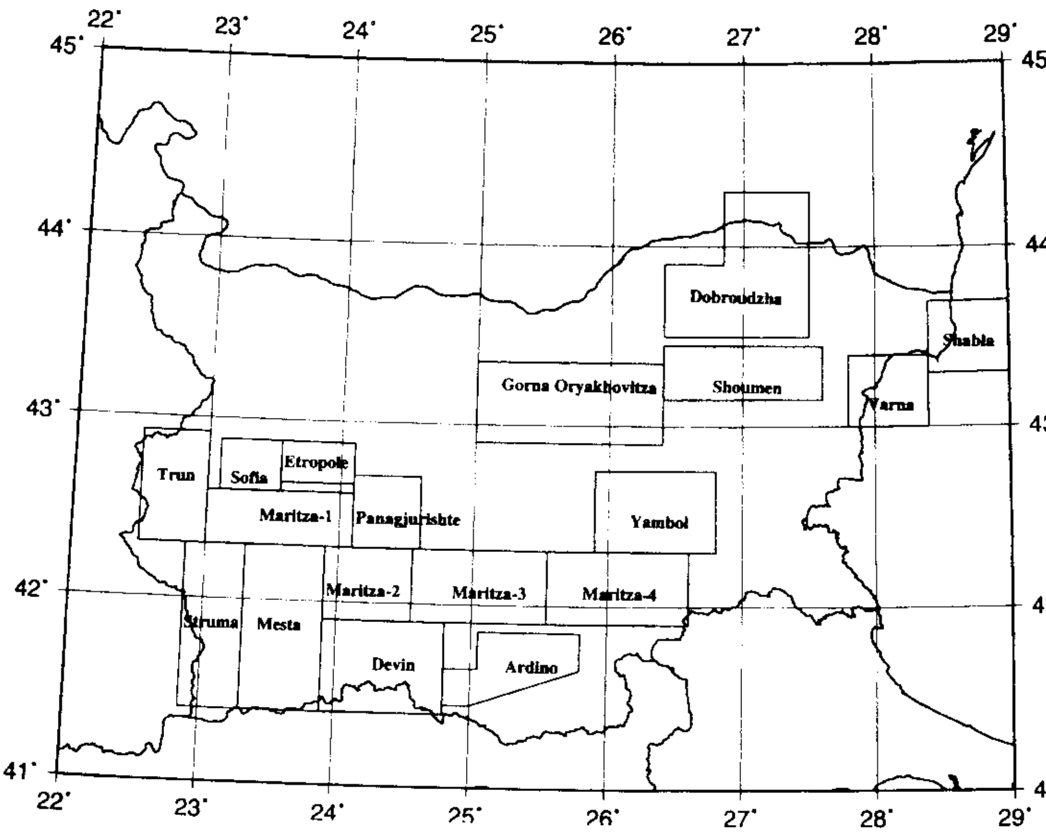


Fig. 3. Seismogenic zones in Bulgaria (after Orozova-Stanishkova and Slejko, 1994).

Orozova-Stanishkova and Slejko (1994) proposed a seismic zoning of Bulgaria consisting of 16 seismogenic areas. These authors give a detailed description of the parameters for each zone, which have been used, slightly revised (Fig. 3), also in this paper. The revision consisted in a reduction of the spatial extension of some of the zones, according to the epicentral distribution of their seismicity.

The *earthquake catalogue*, used for the analysis of the seismicity, is described and analyzed in detail in Stanishkova and Slejko (1991) and Orozova-Stanishkova and Slejko (1994). The size of the quakes is given in terms of surface wave magnitude, $M_s$, while the completeness of the catalogue can be estimated by looking at Fig. 4. The catalogue covers the period 28 A.C. – 1990 but it can be considered fairly complete for magnitudes greater than 4 only for this century. Furthermore, only the main shocks of the whole catalogue time span have been considered; their aftershocks have been removed according to the algorithm suggested by Keilis-Borok et al. (1980).

In the parametrization of the *seismic source* the focal mechanisms define the double-couple orientation, while the seismogenic areas and the earthquake catalogue are used to define the spatial distribution. The procedure to assign a seismic moment to each source is discussed in the next chapter. The next chapter also describes how the above data set is used as input data for computing synthetic seismograms.

## 3. Calculations

In order to account for the spatial and magnitude uncertainties existing in each earthquake catalogue, and to obtain, therefore, a more reliable distribution of the maximum observed magnitude over the Bul-

Fig. 4. Magnitude–time distribution of the Bulgarian earthquakes with magnitude larger than 3.6: (a) for the period 1400–1989; (b) for the period 1850–1989.

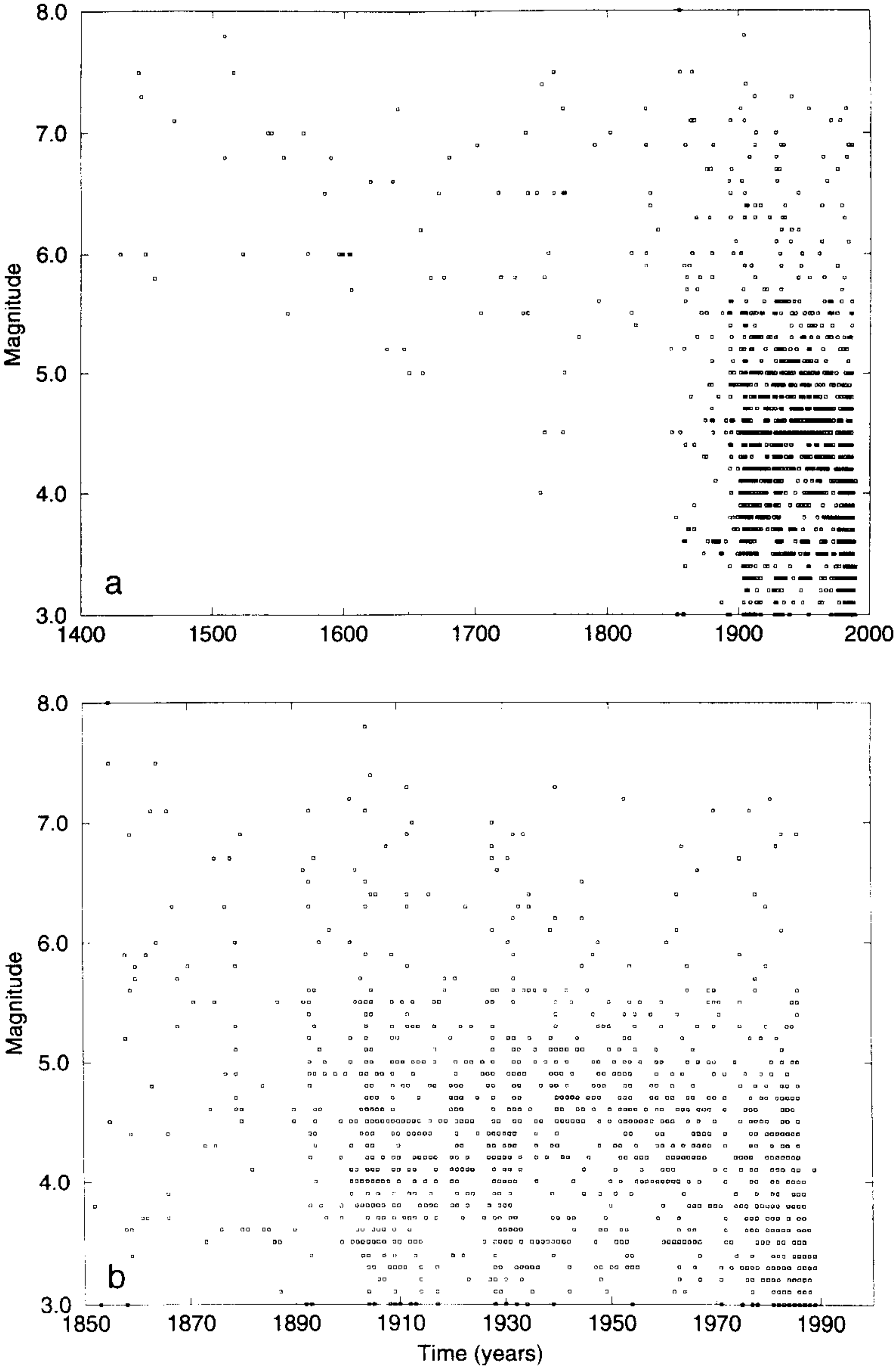
8.0
7.0
6.0
5.0
4.0
3.0
Magnitude
a
1400
1500
1600
1700
1800
1900
2000
b
1850
1870
1890
1910
1930
1950
1970
1990
Time (years)

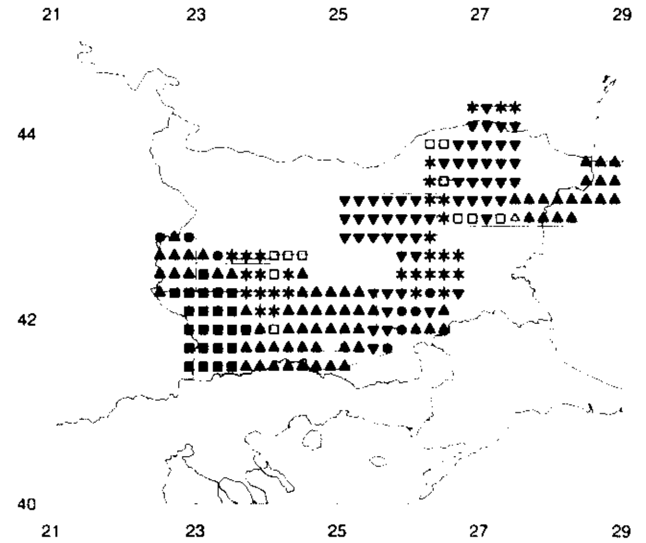


Fig. 5. Representation of the "smoothed" seismicity in each seismogenic zone.

| Magnitude | |
|---|---|
| ■ | 7.50–8.00 |
| ▲ | 7.00–7.50 |
| ▼ | 6.50–7.00 |
| • | 6.00–6.50 |
| * | 5.50–6.00 |
| □ | 5.00–5.50 |
| △ | –5.00 |

garian territory, the seismicity is discretized and "smoothed". First, the area is subdivided into 0.2° × 0.2° cells and the magnitude of the strongest earthquake occurred within a cell is assigned to it. In this process of discretization of the seismicity, it was however found that not each cell contains a statistically meaningful number of events. Therefore, if a cell contains only small shocks (with magnitude below a certain threshold value), the maximum magnitude to be assigned to that cell is searched through the surrounding ones, applying a smoothing window (Costa et al., 1993). This procedure allows to account for the source dimensions of the largest earthquakes. One can see in Fig. 5, that after the applying of the smoothing window, a large magnitude ($M_s \geq 6.5$) is assigned to the majority of the cells. In the following calculations only the "smoothed" seismicity limited to the seismogenic areas (Fig. 5) is taken into account. In other words, the seismic sources used to generate the synthetic seismograms, are only those which fall within cells located inside a seismogenic zone.

The seismic source is represented by a single double-couple (DC) point source located in the center of each cell. This source replaces all the events falling within the cell. Its "strength" is determined according to the maximum magnitude observed in the cell. The orientation of the double-couple point source is obtained from the available focal-plane solutions, as mentioned before. In the zones where no focal-plane solution is available, the solution available in the nearest zone and best matching the regional tectonic behaviour is considered. The depth of the source was kept constant (10 km) over the whole territory. This depth could be considered as representative for the Bulgarian seismicity (Stanishkova and Slejko, 1991; Orozova-Stanishkova and Slejko, 1994).

When the structural models and the sources are defined, synthetic accelerations are computed using the modal summation technique (Panza, 1985; Panza and Suhadolc, 1987; Florsch et al., 1991) at receivers placed on the grid covering the whole territory under investigation. Notice that the sources and the receivers do not overlap, because the sources are placed in the centre of each cell falling within the seismogenic zones, whereas the receivers are placed at the grid points covering the whole investigated area. In this study the synthetic signals are computed for a maximum frequency of 1 Hz, for which the point-source approximation is assumed to be still acceptable. If shorter periods are to be considered, the finite dimensions of the fault cannot be neglected and the rupturing process at the source has to be defined.

To reduce the number of computed seismograms, the source–receiver distance is kept below an upper threshold, which is considered to be function of the magnitude associated to the source (Costa et al., 1993). The maximum source–receiver distance has been set equal to 25, 50 and 90 km for $M < 6$, $6 \leq M \leq 7$ and $M > 7$, respectively. At each receiver the P-SV (radial components) and SH (transverse component) are estimated. The horizontal components are first rotated to a common reference system (NS- and EW-directions) and then their vector sum is calculated.

Synthetic seismograms are originally computed for a seismic moment of $10^{-7}$ Nm, the amplitudes being successively properly scaled according to the (smoothed) magnitude associated with the cell of the source. In fact, keeping the magnitude constant within each zone leads to an over-estimation of the seismicity for the larger seismogenic areas. The scalar seismic moments are derived from magnitude using the relation of Kanamori and Anderson (1975). Source finiteness is accounted for by properly weighting the source spectrum in the frequency domain using the curves proposed by Gusev (1983). We have chosen to use the Gusev curves in the present study due to the following reasons: On one hand, Vaccari (1995) has found that in order to fit with synthetic accelerations the observed amplitudes of strong ground motion records in the case of the Irpinia, 1980, earthquake (e.g. Westaway and Jackson, 1987; Bernard and Zollo, 1989), he had to scale the point-source synthetic spectra by multiplying them with the Gusev (1983) proposed spectra in order to account for the correct corner frequency. On the other hand the Gusev displacement spectra show a "sag" for periods longer than about 2 s, but a "rise" for periods from 2 s to 0.1 s, as compared to the $\omega^{-2}$ spectra (e.g. Joyner, 1984; Houston and Kanamori, 1986). Since we compute accelerations for periods down to 1 s, the maximum peak of the point-source synthetics is usually between 2 s and 1 s. In this range the Gusev spectra slightly overestimate the $\omega^{-2}$ ones for large earthquakes, leading to a slightly bigger maximum peak in the synthetics. We have, therefore, decided to scale our synthetics with the Gusev spectra to be "conservative" in our estimates and consider the worst possible scenario.

The maximum ground acceleration (AMAX) has been chosen as the parameter representing the strong ground motion and, consequently, the seismic hazard. However, since acceleration time histories are computed at each grid point, it is also possible to consider other parameters, like Arias (1970) intensity or other integral quantities, which could be of interest in seismic engineering. In the present study, only

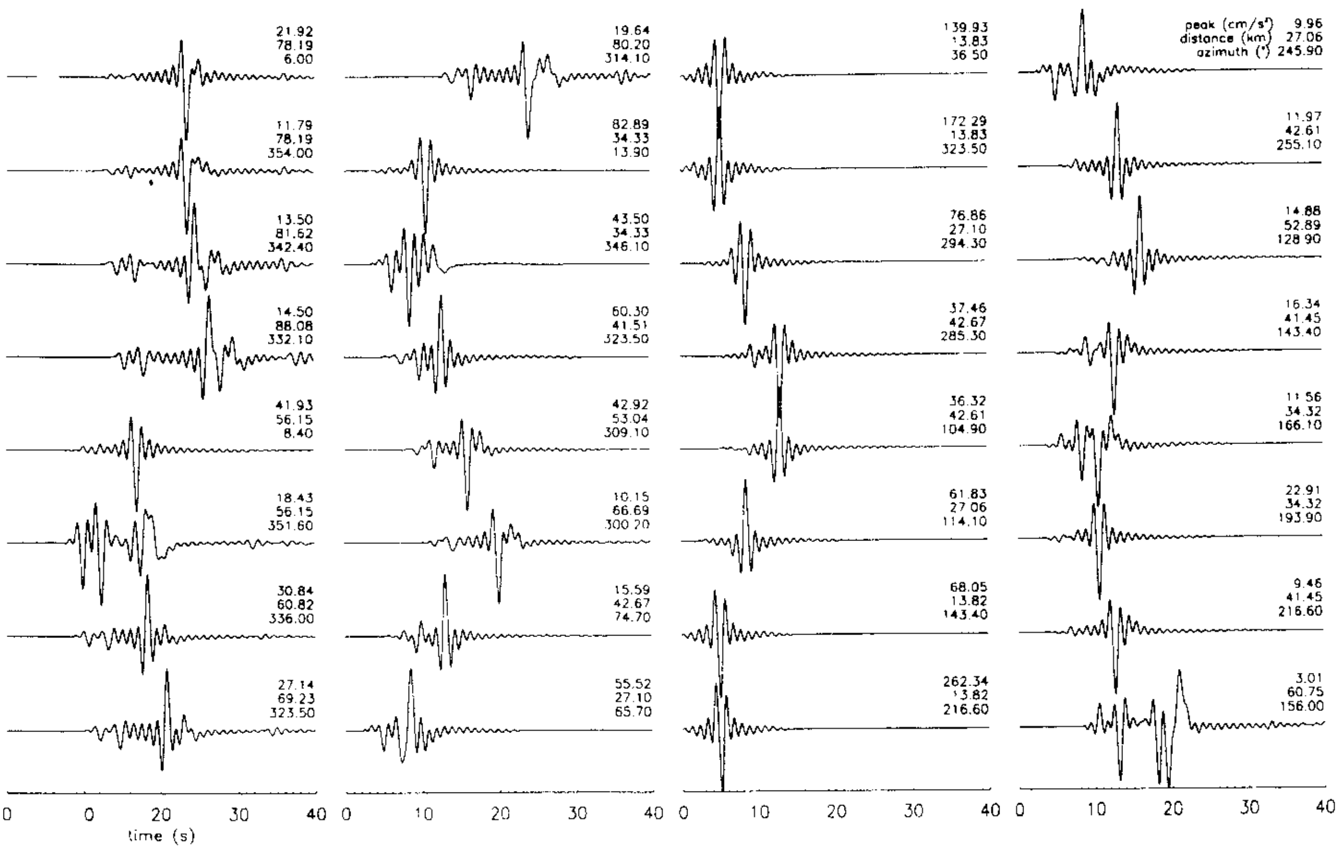


Fig. 6. Complete set of accelerograms computed at the receiver (42.4°N, 23°E) with the highest AMAX (see Fig. 7) among the study region. The numbers reported in the right upper corner of each accelerogram are (from the top to the bottom): the peak value (expressed in cm/s²), the source–receiver distance (in km) and the azimuth (in degrees) of the source–receiver line.

the maximum value of the AMAX at each receiver is considered in the hazard analysis and plotted on a map.

The complete set of accelerograms computed at the receiver (42.4°N, 23°E), related to the site where the maximum value of AMAX has been obtained, is shown in Fig. 6. Each accelerogram in the set corresponds to a source, placed on a grid point around the receiver according to the source–receiver distance criteria discussed above. Every trace in Fig. 6 represents the maximum among the components N–S and E–W of the relative accelerogram. The numbers reported in the right upper corner of each accelerogram are (from the top to the bottom): the peak value (expressed in $cm/s^2$), the source–receiver distance (in km) and the azimuth (in degrees) of the source–receiver line. The peak values of the accelorogram set range from 3.01 to 262.34 $cm/s^2$. The maximum peak (262.34 $cm/s^2$) comes from a source in the Struma zone, placed at 13.82 km from the receiver site.

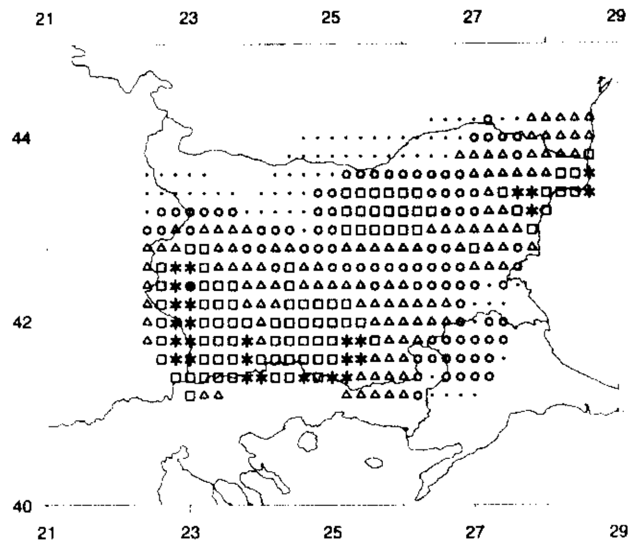


Fig. 7. AMAX calculated in Bulgaria. The values are expressed in g.

| | |
|---|---|
| ● | 0.30–0.40 |
| * | 0.20–0.30 |
| □ | 0.10–0.20 |
| Δ | 0.05–0.10 |
| ο | 0.02–0.05 |
| . | –0.02 |

## 4. Results

The final results are given in Fig. 7, AMAX being expressed hereafter in units of g.

The intensity–acceleration relation (Table 3) proposed by Voutkov et al. (1986) can be used to compare the computed maximum accelerations with the macroseismic intensities (the only available parameter related to historical data) and with the seismic hazard results derived by other methods and expressed in terms of intensity.

The highest values of AMAX (0.3–0.4 g, intensity IX–X according to Table 3) are obtained in southwestern Bulgaria (on the boundary between the Struma, Maritza and Trun zones). High AMAX values (0.2–0.3 g, intensity VIII–IX according to Table 3) are calculated in the Trun, Struma, Mesta, Devin, Ardino zones, as well as in the northeastern part of the country (Varna and Shabla zones). Sofia, Maritza and Gorna Oryakhovitza zones are characterized by AMAX values of the order of 0.1–0.2 g. The remaining parts of the country are characterized by AMAX values less than 0.05 g. The northwestern and southeastern parts of Bulgaria are thus estimated to be the less dangerous zones with AMAX values below 0.02 g (i.e. less than intensity V according to Table 3).

It should be mentioned that the biggest Bulgarian cities with relevant economical and cultural importance, such as Sofia, Plovdiv and Varna are all situated in the zones with high seismic hazard. The values of AMAX calculated there are about 0.1–0.2 g (intensity VII–VIII, see Table 3).

Table 3
Acceleration–intensity relation after Voutkov et al. (1986)

| Intensity | Acceleration | |
|---|---|---|
| | ($cm/s^2$) | (g) |
| XII | 850.8 | 0.87 |
| XI | 650.4 | 0.66 |
| X | 444.8 | 0.45 |
| IX | 275.3 | 0.28 |
| VIII | 155.6 | 0.16 |
| VII | 80.9 | 0.08 |
| VI | 38.9 | 0.04 |
| V | 17.4 | 0.02 |
| IV | 7.3 | 0.01 |

## 5. Discussion and conclusions

An advantage of the deterministic approach used in this study is that the values of AMAX are estimated starting from the seismic moment. The results obtained by this method are specially useful for large constructions, which have a response spectrum peaked at values below 1 Hz. The deterministic method allows also to easily include new information made available after the stage at which the hazard analysis was carried out, and to assess the influence of these new data. The described deterministic method is currently being improved by incorporating into it an estimate of the probability of occurrence of different AMAX based on the recurrence time of events of different magnitude and different seismogenic zones.

Some limitations of the present study are connected to the strong approximations introduced into the definition of the structural models. More precisely, the velocity models used to describe the structure in the different polygons are very crude, the seismic wave velocity attenuation relations used were those appropriate for Italy and not for Bulgaria. Further efforts are also necessary to get high-quality focal plane solutions in each seismogenic zone. Generally, with the deterministic methods it is not possible to take into account the uncertainties associated with estimates of ground motion and maximum magnitude, unless extensive parametric analyses are performed.

The estimation of AMAX obtained in this paper takes into account only the Bulgarian seismicity. The influence on the seismic hazard on the Bulgarian territory of the seismicity of the surrounding countries, such as Greece, Turkey, former Yugoslavia and Romania was not investigated here. It should be mentioned that the seismic hazard of northeastern Bulgaria for example, is influenced by the Vrancea (Romania) intermediate-depth seismicity (Orozova-Stanishkova and Slejko, 1994), which was neglected in this study. The influence of these external sources on the seismic hazard of Bulgaria will be investigated in a future study.

In order to compare the results, obtained by using a deterministic seismic hazard assessment (hereafter

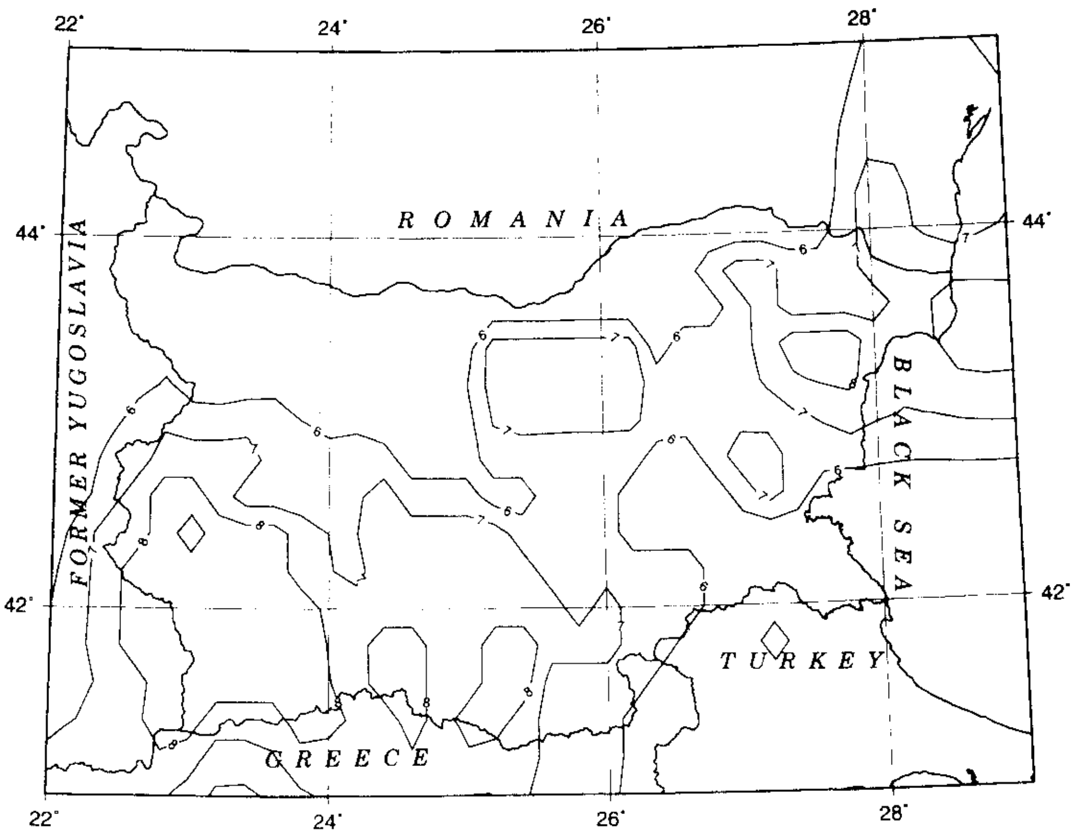


Fig. 8. Map of the intensity, obtained from the values of AMAX (Fig. 7), according to Table 3.

referred to as DSHA) with those, obtained by using a probabilistic seismic hazard assessment (hereafter referred to as PSHA) approaches in Bulgaria, we have constructed a seismic hazard map in terms of intensity (Fig. 8). We have converted the AMAX values into intensity according to the Table 3. A map to which we can compare our results is given in Fig. 9, which represents the seismic hazard of Bulgaria obtained by using PSHA (Orozova-Stanishkova and Slejko, 1994) methods. Many features in both figures are quite similar: the most dangerous part is southwestern Bulgaria, the less dangerous are the northwestern and the southeastern parts of the country, the remaining areas showing a fairly uniform medium-level hazard. However, some differences are worth to be mentioned: the AMAX values in the central part of southernmost Bulgaria (Devin and Ardino zones) and around the town of Varna in northeastern Bulgaria (0.2–0.3 g, corresponding to intensity VIII–IX according to Table 3, see Fig. 8) estimated with the DSHA are higher than those obtained by the PSHA (forecast intensity around VII, according to Orozova-Stanishkova and Slejko, 1994, see Fig. 9) methods. Such differences can be explained by the fact that in the DSHA, presented here, we have used the whole catalogue span (28 A.D.–1990), while in the PSHA only the seismicity of the period 1800–1988 is considered in the calculations (Orozova-Stanishkova and Slejko, 1994). In such a way some large earthquakes (for example those of magnitude 7.5, which affected the town of Varna in 542 and 1444) are not used, or used with very low probability as maximum expected earthquake in the procedure for PSHA. The values of the "probabilistic" seismic hazard (intensity VIII–IX), calculated in the Gorna Oryakhovitza and Maritza zones (the central parts of northern and southern Bulgaria, see Fig. 9) is higher than those obtained by the DSHA (AMAX 0.1–0.2 g, corresponding to intensity VII–VIII, according to Table 3, see Fig. 8). These differences are due to the fact, that in the PSHA method calculations seismogenic lines were used, which "concentrate" the

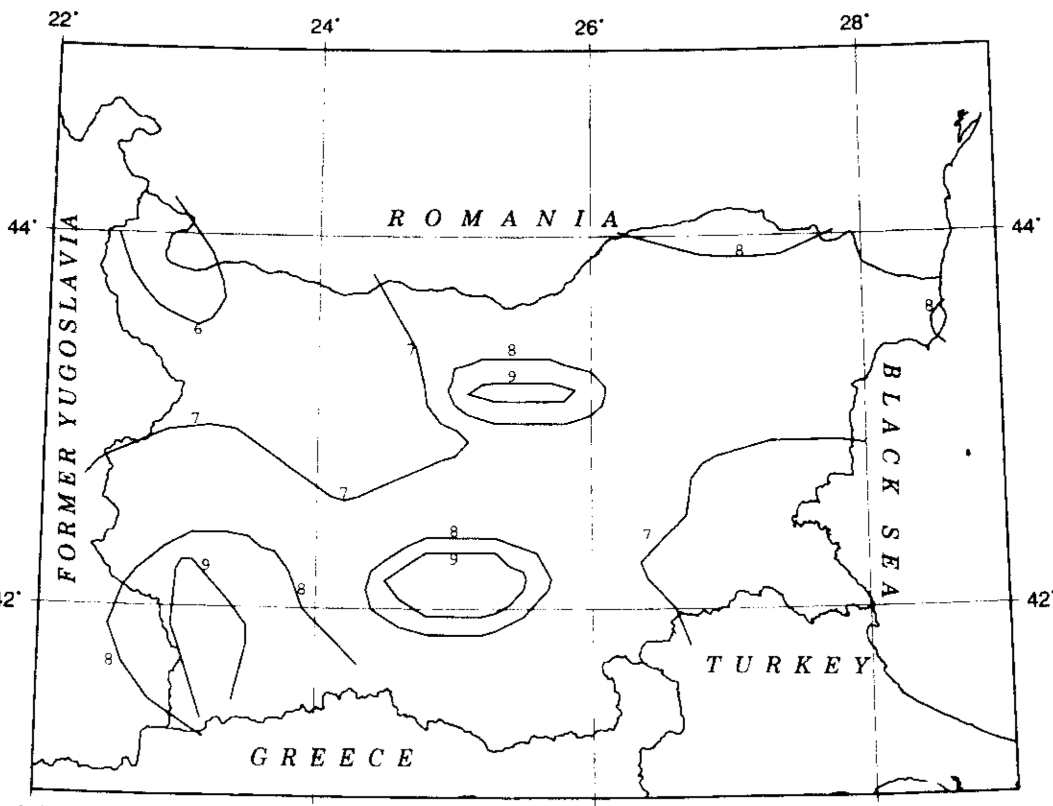


Fig. 9. Map of the maximum expected intensity at 37% level of nonexceedence in 100 yr (modified from Orozova-Stanishkova and Slejko, 1994). This hazard map is obtained with probabilistic methods.

maximum hazard. We have also to remember, that the differences in North Bulgaria are also due to the fact that we have not considered in this study the seismicity of the surrounding countries, as it was already mentioned.

The shakeability map of Bulgaria, proposed by Bonchev et al. (1982), for a 1000 year period reveals a maximum intensity IX in the southwestern and northeasternmost parts of the country, intensity VIII in the central part, and intensity VII elsewhere. The probability of occurrence of earthquakes with magnitude over 6.8 in Bulgaria, evaluated in Reisner (1988), is one in the southwestern, the central and northeasternmost parts of the country. These results seem to be confirmed by the computations done in this paper using the deterministic seismic hazard assessment.

## Acknowledgements

I. Orozova-Stanishkova, undertook this work at the Institute of Geodesy and Geophysics (now Department of Earth Sciences) of the University of Trieste, Italy, financially supported by the "Human Capital and Mobility – GO WEST Programme", grant no. 3480 of the Commission of the European Communities. Further financial support for this research came also from the Commission of European Communities Programme Environment and Climate, Area 4.1.1 Seismic Hazard Project "Long-Period Seismic Risk" (contract no. EV5V-CT94-0491/DG12SOLS), the Commission of European Communities Programme COPERNICUS "Quantitative Seismic Zoning of the Circum-Pannonian Region" (contract No. CIPA-CT94-0238) and Italian CNR contracts 92.02867.PF54 and 93.02481.PF54. The authors are very grateful to the reviewers, Prof. R. Madriaga and Prof. Z. Wang, for the critical and very helpful comments.

## References

Arias, A., 1970. A measure of earthquake intensity. In: R. Haunsen (Editor). Seismic Design for Nuclear Power Plants. Cambridge, MA, pp. 438–483.

Bernard, P. and Zollo, R., 1989. The Irpinia (Italy) 1980 earthquake: detailed analysis of a complex normal faulting. J. Geophys. Res., 94: 1631–1647.

Bonchev, E., Bune, V.I., Christoskov, L., Karajuileva, J., Kostadinov, V., Reisner, G.I., Rizhikova, S., Shebalin, N.V., Sholpo, V.N. and Sokerova, D., 1982. A method for compilation of seismic zoning prognostic maps for the territory of Bulgaria. Geol. Balcanica, 12.2: 3–48.

Cornell, C.A., 1968. Engineering seismic risk analysis. Bull. Seismol. Soc. Am., 58: 1583–1606.

Costa, G., Panza, G.F., Suhadolc, P. and Vaccari, F., 1993. Zoning of the Italian territory in terms of expected peak ground acceleration derived from complete synthetic seismograms. In: Proc. School Geophys. Explor. Areas Complex Geology, Erice 1992. J. Appl. Geophys., 30: 149–160.

Dachev, Hr. and Volvovsky, I.S., 1985. Deep structure of Bulgaria along the Petrich–Nikopol EMCM-DSS Traverse. Boll. Geofis. Teor. Appl., 108: 263–278.

Dotzev, N. and Yunga, S., 1988. Focal mechanisms of earthquakes in Bulgaria. Izv. Earth Phys., 24: 247–253.

Florsch, N., Faeh, D., Suhadolc, P. and Panza, G. F., 1991. Complete synthetic seismograms for high-frequency multimode SH waves. In: A. Udias and E. Buforn (Editors), El Escorial Workshop Proceedings. Pageoph, 136: 529–560.

Gumbel, E. J., 1966. Statistics of Extremes. Columbia University Press, New York, 355 pp.

Gusev, A. A., 1983. Descriptive statistical model of earthquake source radiation and its application to an estimation of short period strong motion. Geophys. J. R. Astron. Soc., 74: 787–800.

Houston, H. and Kanamori, H., 1986. Source spectra of great earthquakes: teleseismic constraints on rupture process and strong motion. Bull. Seismol. Soc. Am., 76: 19–42.

Joyner, W., 1984. A scaling law for the spectra of large earthquakes. Bull. Seismol. Soc. Am., 74: 1167–1188.

Kanamori, H. and Anderson, D., 1975. Theoretical basis of some empirical relations in seismology. Bull. Seismol. Soc. Am., 65: 1073–1095.

Keilis-Borok, V., Knopoff, L., Rotwain, I. and Sidorenko, T., 1980. Bursts of seismicity as long-term precursors of strong earthquakes. J. Geophys. Res., 85: 803–812.

Orozova-Stanishkova, I., and Slejko, D., 1994. Seismic hazard of Bulgaria. Nat. Hazards, 9: 247–271.

Panza, G. F., 1985. Synthetic seismograms: The Rayleigh waves model summation. J. Geophys., 58: 125–145.

Panza, G. F. and Suhadolc, P., 1987. Complete strong motion synthetics. In: B.A. Bolt (Editor), Seismic Strong Motion Synthetics. Computational Techniques 4. Academic Press, Orlando, pp. 153–204.

Reisner, G.I. (Editor), 1988. Long-term seismic hazard prognosis upon geologo-geophysical data complex. Nauka, Moscow, 112 pp. (in Russian)

Shanov, S. and Georgiev, Tz., 1992. The January 23, 1984 Pavlikeni earthquake and its seismotectonic interpretation. J. Bulg. Geol. Soc., 53(1): 85–90 (in Bulgarian).

Shanov, S. and Kostadinov, I., 1992. Configuration of the deep geophysical discontinuities beneath the territory of Bulgaria. Geol. Balcanica, 22(2): 71–79.

Shanov, S., Spassov, E. and Georgiev, Tz., 1992. Evidence for the existence of a paleosubduction beneath the Rhodopean massif (Central Balkans). Tectonophysics, 206: 307–314.

Sokerova, D. and Velichkova, S., 1989. Velocity characteristics of the Earth's crust in Bulgaria. Gerlands Beitr. Geophys., 98(5): 398–408.

Solakov, D.E. and Simeonova, S.D. (Editors), 1993. Bulgaria Catalogue of Earthquakes 1981–1990. Bulgarian Academy of Sciences, Sofia, 40 pp.

Stanishkova, I. and Slejko, D., 1990. The 1986 Strazhitza earthquake sequences within the contest of the seismicity of Bulgaria. In: Atti 9-o Convegno Nazionale GNGTS, Esagrafica, Roma, pp. 177–188.

Stanishkova, I. and Slejko, D., 1991. Some seismotectonic characteritics of Bulgaria. Boll. Geofis. Teor. Appl., 33: 187–210.

Vaccari, F., 1995. LP-displacement hazard evaluation in Italy. In: Proc. 24th General Assembly of the European Seismological Commission, Athens, 3: 1489–1498.

Voutkov, V., Chanov, St. and Demirev, A., 1986. Evaluation de l'intensite et de l'accelaration maximale en zones seismiques. Geol. Appl. Idrogeol., 21(1): 13–22.

Westaway, R. and Jackson, J., 1987. The earthquake of 1980 November 23 in Campania — Basilicata (southern Italy). Geophys. J. R. Astron. Soc., 90: 375–443.

## Figure 14

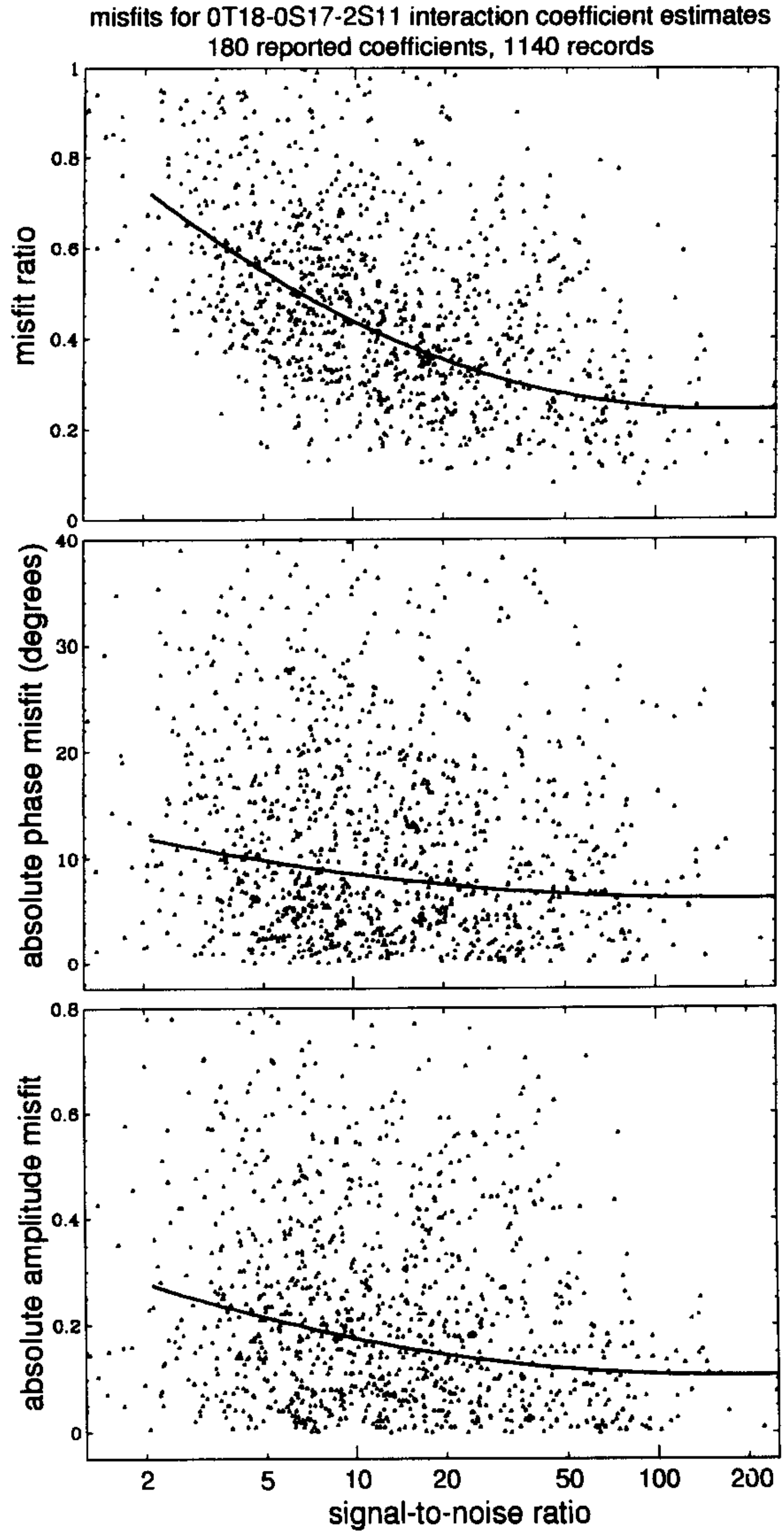

misfits for 0T18-0S17-2S11 interaction coefficient estimates
180 reported coefficients, 1140 records
misfit ratio
0
0.2
0.4
0.6
0.8
1
absolute phase misfit (degrees)
0
10
20
30
40
absolute amplitude misfit
0
0.2
0.4
0.6
0.8
2
5
10
20
50
100
200
signal-to-noise ratio

# Figure 15

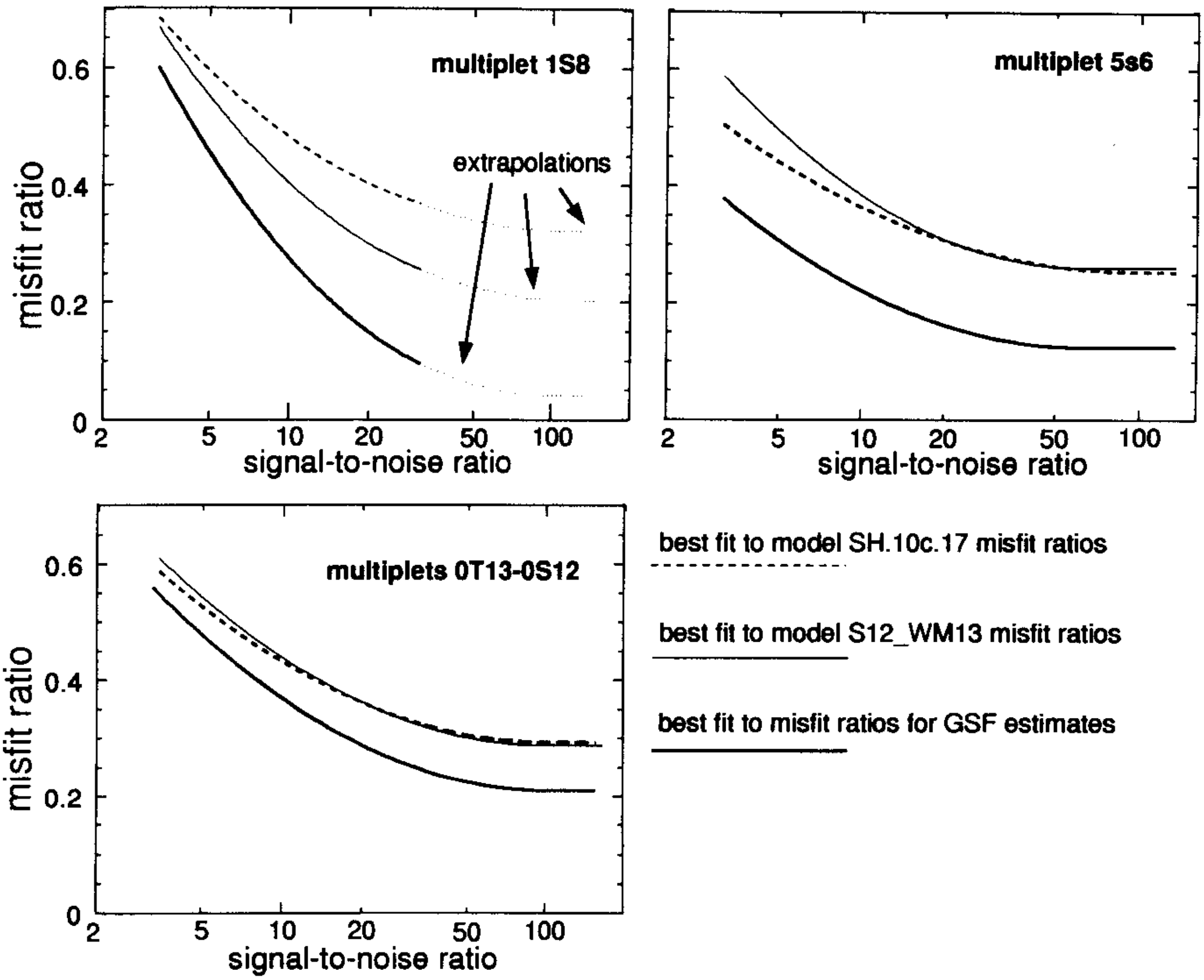
multiplet 1S8
extrapolations
multiplet 5s6
multiplets 0T13-0S12
misfit ratio
signal-to-noise ratio
0
0.2
0.4
0.6
2
5
10
20
50
100
best fit to model SH.10c.17 misfit ratios
best fit to model S12_WM13 misfit ratios
best fit to misfit ratios for GSF estimates

# Figure 16

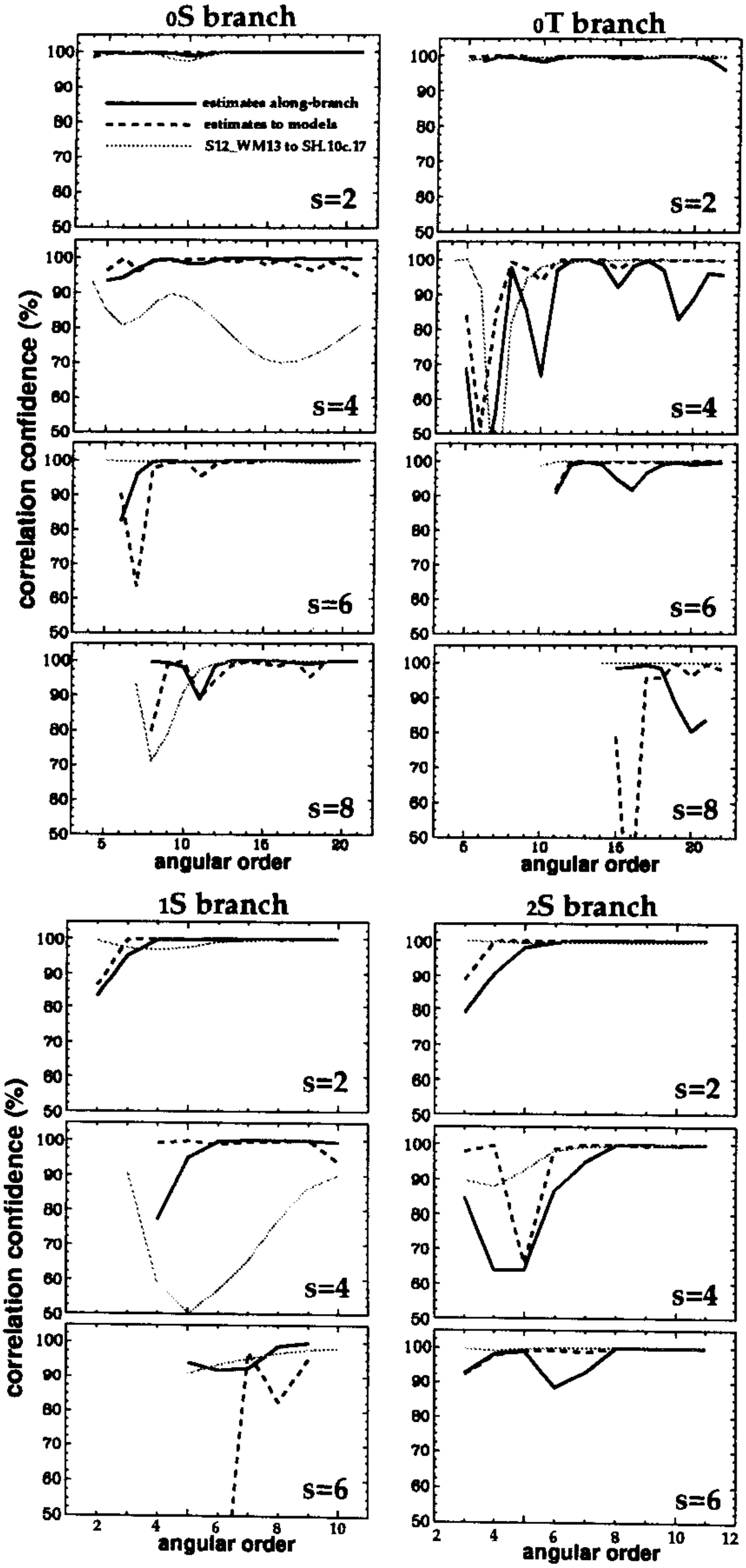
0S branch
0T branch
1S branch
2S branch
estimates along-branch
estimates to models
S12_WM13 to SH.10c.17
correlation confidence (%)
angular order
s=2
s=4
s=6
s=8

**Figure 17**

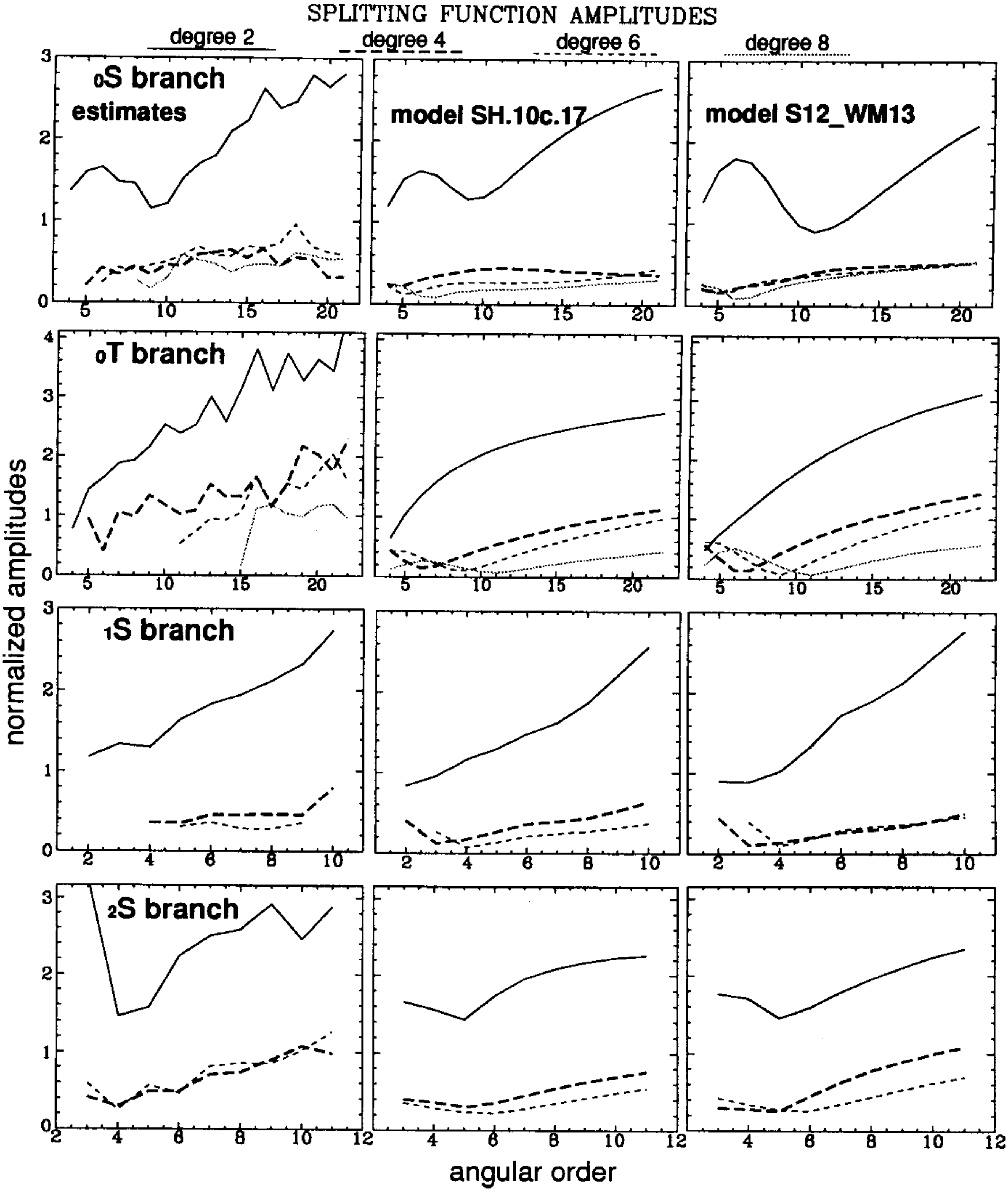

SPLITTING FUNCTION AMPLITUDES
degree 2
degree 4
degree 6
degree 8
0S branch
estimates
model SH.10c.17
model S12_WM13
0T branch
1S branch
2S branch
normalized amplitudes
angular order

**Figure 18**

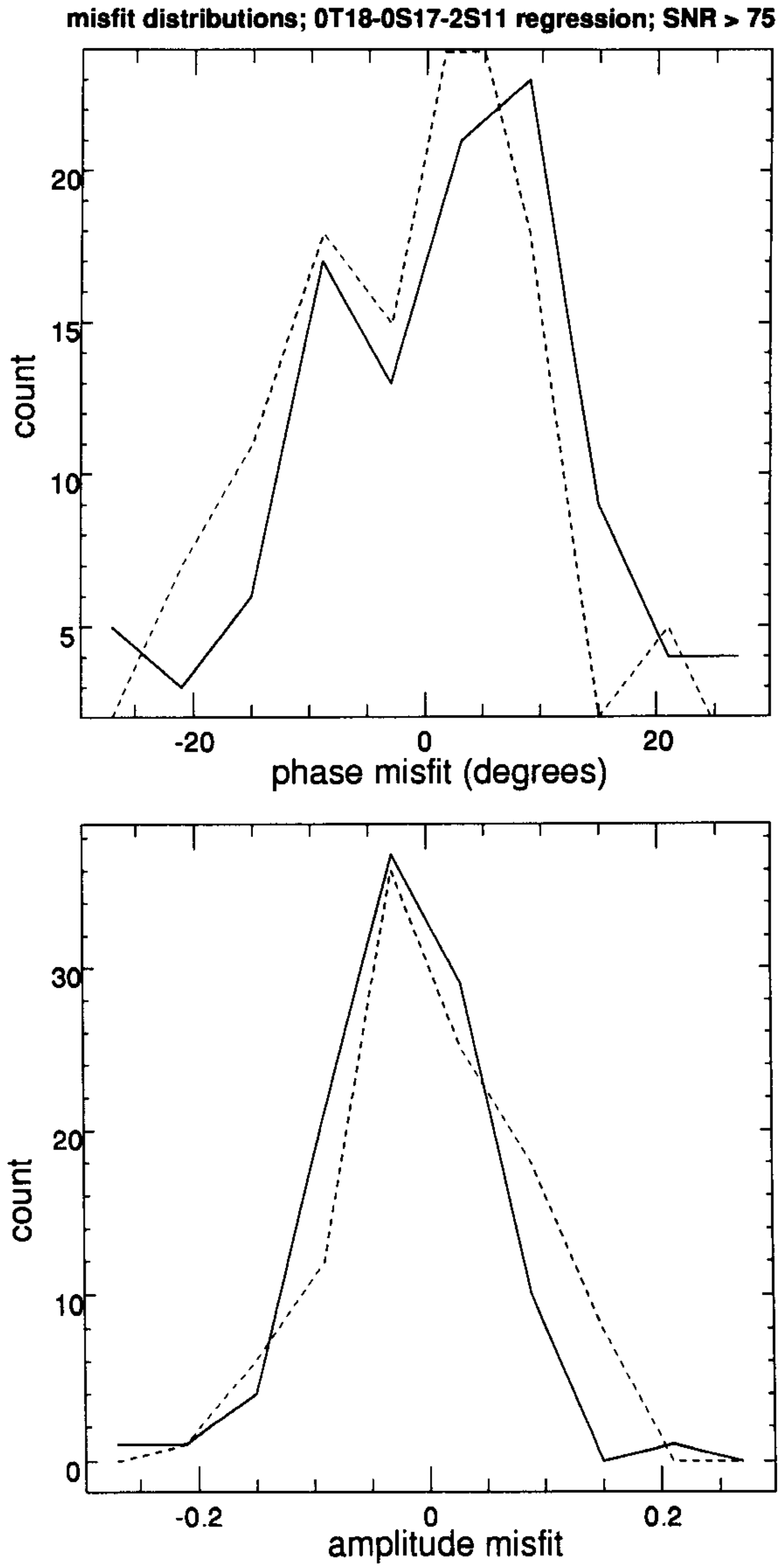
misfit distributions; 0T18-0S17-2S11 regression; SNR > 75
count
20
15
10
5
-20
0
20
phase misfit (degrees)
count
30
20
10
0
-0.2
0
0.2
amplitude misfit

**Figure 19**

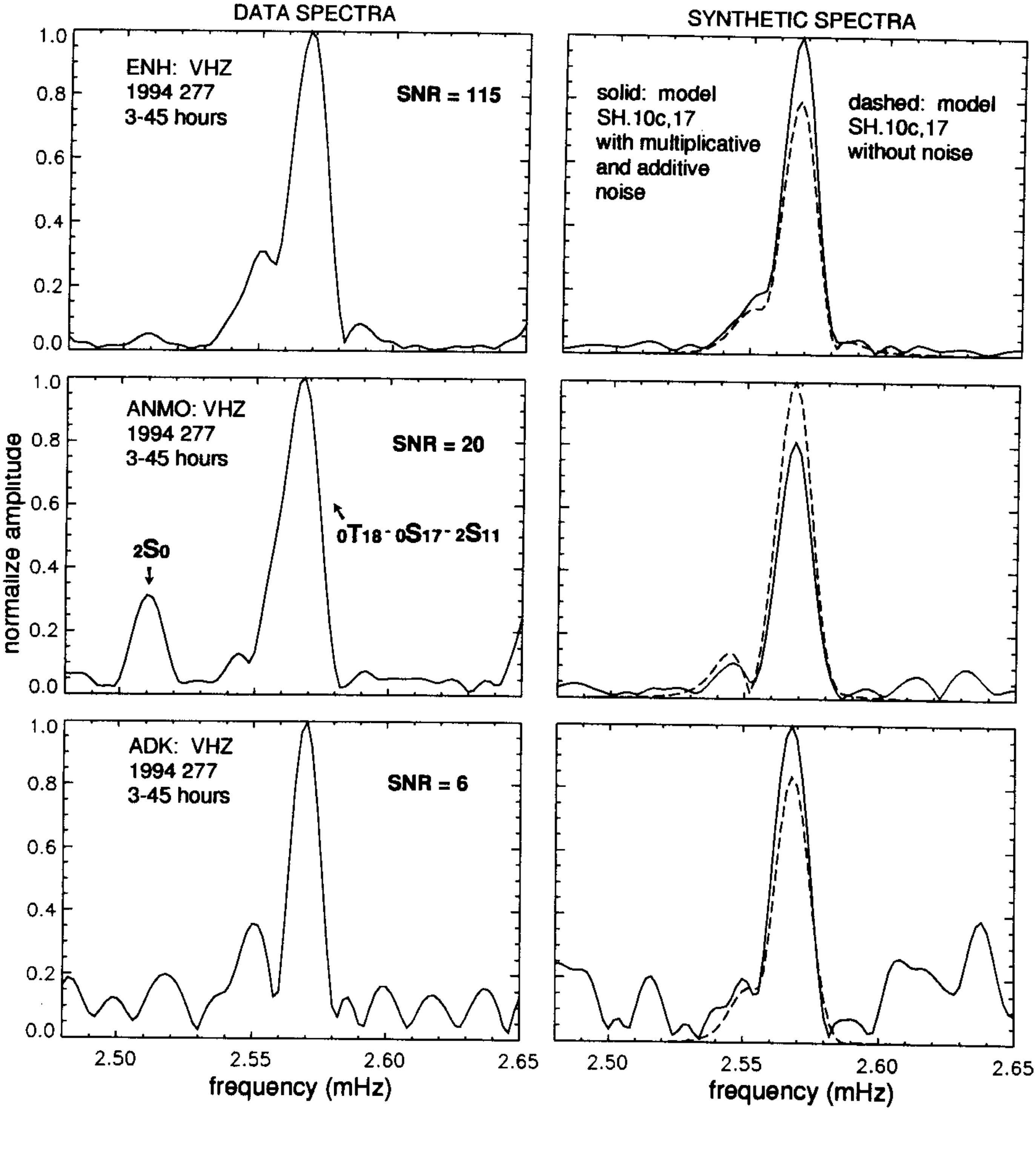

DATA SPECTRA
SYNTHETIC SPECTRA
ENH: VHZ
1994 277
3-45 hours
SNR = 115
solid: model
SH.10c,17
with multiplicative
and additive
noise
dashed: model
SH.10c,17
without noise
ANMO: VHZ
1994 277
3-45 hours
SNR = 20
$_2S_0$
$_0T_{18}$ - $_0S_{17}$ - $_2S_{11}$
ADK: VHZ
1994 277
3-45 hours
SNR = 6
normalize amplitude
1.0
0.8
0.6
0.4
0.2
0.0
2.50
2.55
2.60
2.65
frequency (mHz)

**Figure 20**

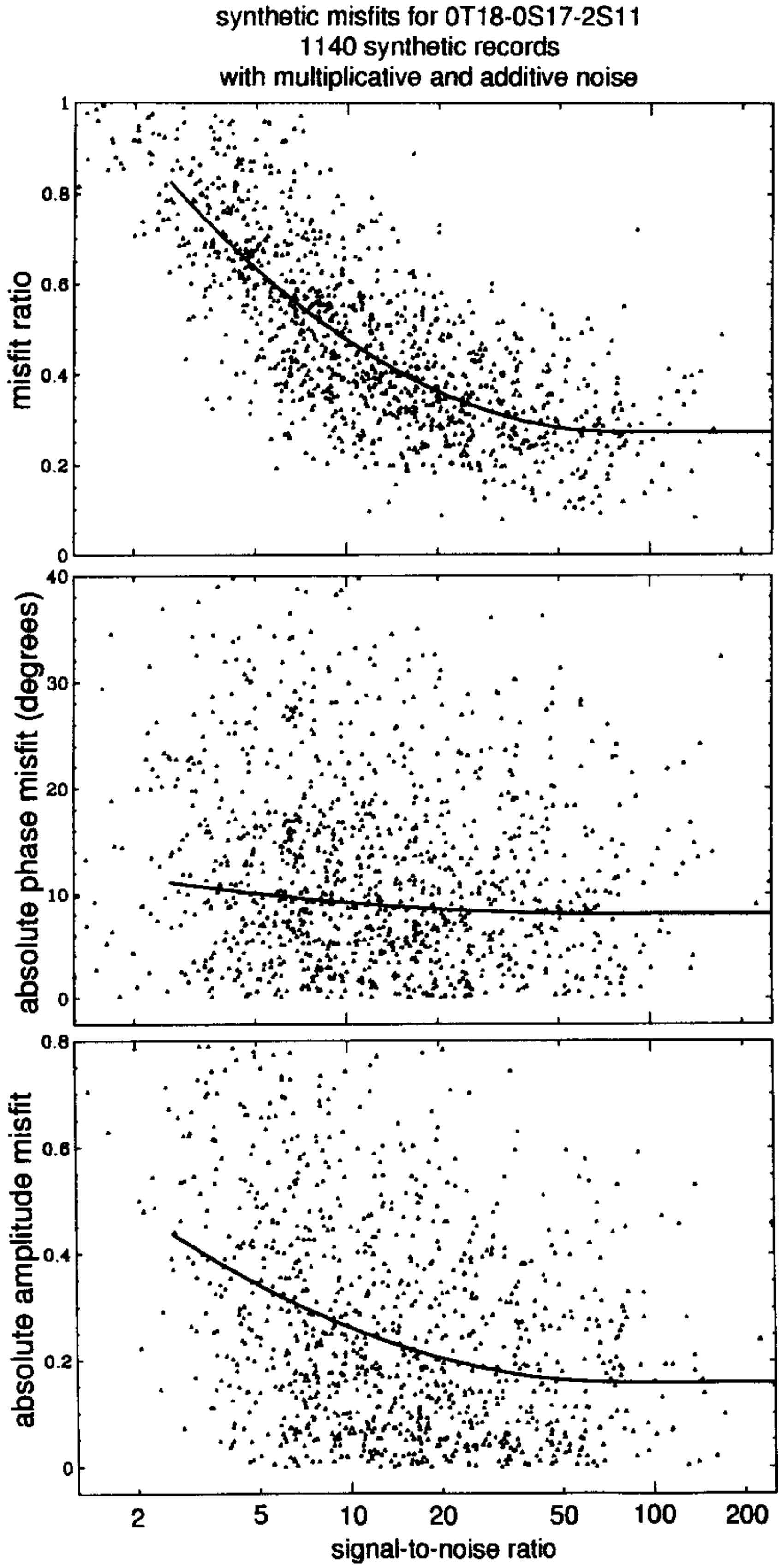
synthetic misfits for 0T18-0S17-2S11
1140 synthetic records
with multiplicative and additive noise
misfit ratio
1
0.8
0.6
0.4
0.2
0
absolute phase misfit (degrees)
40
30
20
10
0
absolute amplitude misfit
0.8
0.6
0.4
0.2
0
2
5
10
20
50
100
200
signal-to-noise ratio